2013-09-13

Spallation in Dual-Shock Quark Nova: A Robust Nucleosynthetic Process

Ouyed Hernandez, Amir Hassan

UNIVERSITY OF CALGARY

Spallation in Dual-Shock Quark Nova: A Robust Nucleosynthetic Process

by

Amir Hassan Ouyed Hernandez

A THESIS

SUBMITTED TO THE FACULTY OF GRADUATE STUDIES

IN PARTIAL FULFILLMENT OF THE REQUIREMENTS FOR THE

DEGREE OF MASTER OF SCIENCE

DEPARTMENT OF PHYSICS AND ASTRONOMY

CALGARY, ALBERTA

SEPTEMBER, 2013

Abstract

This thesis presents an alternate, spallation, nucleosynthesis mechanism in the context of the dual-shock Quark Nova (dsQN). The dsQN is an evolutionary channel where a core collapse supernova is followed by the detonation of its neutron star - an event that generates nuclear spallation reactions. Spallation produces new, daughter isotopes, by the fragmentation of larger nuclei - in contrast to conventional nucleosynthesis models which are based on the accretion of smaller nuclei and particles into larger nuclei. This spallation nucleosynthesis model is fairly extensive - it can produce abundant isotopes in the $A < 130$ mass range and therefore solve some of the issues faced by conventional r-process models. Furthermore, the specificities of dsQN spallation might be the key to explain the peculiarities of ^{44}Ti production in the universe. Finally, dsQN spallation nucleosynthesis is fairly robust in relation to the universe's age and the chemical composition of core-collapse supernovae.

Acknowledgements

I want to first thank my mentor and advisor Dr. Rachid Ouyed. He gave me engaging and original projects that materialized into this thesis. His comments and insights were invaluable, and he spent countless hours supervising and engaging my work. Finally, he was not only crucial for my academic development, but also helped me make Calgary a home.

I want to thank my co-advisor Dr. Denis Leahy. He gave my work plenty of fair and constructive criticism. He collaborated in all the papers that were included in this dissertation. I want to also thank Dr. Prashanth Jaikumar, who was also a collaborator in one of the papers.

Finally, I want to thank my parents, who always supported enthusiastically my life-choices. Their support has been invaluable.

Table of Contents

List of Tables

List of Figures and Illustrations

List of Symbols, Abbreviations and Nomenclature

Symbol	Definition
U of C	University of Calgary
QN	Quark Nova
dsQN	dual-shock Quark Nova
SN	Supernova
cc-SN	core collapse Supernova
QGP	Quark Gluon Plasma
QS	Quark Star
NSM	Neutron Star Merger

Chapter 1

Introduction

Usually, the picture of nucleosynthesis in lecture halls and textbooks is presented as complete. The Big Bang created hydrogen, helium, and other light elements, and stars burn these elements into nuclei as heavy as iron. Finally, neutron capture processes inside old stars and supernovae create all the elements heavier than iron.

The truth is that there are fundamental problems with this conventional narrative of nucleosynthesis. The core-collapse supernova, which is the prime candidate for the rapid-neutron capture process (r-process), is incompletely understood. Existing simulations of the supernova are only able to detonate it under very limiting conditions (Burrows, 2013), and are unable to recreate the conditions necessary for the r-process to take place. Without a picture of the r-process, half of the solar abundances are left unexplained.

Furthermore, there are inconsistencies between theory and observation in regards to ^{44}Ti in core-collapse supernovae. These inconsistencies could signal a deeper flaw in the explosive nucleosynthesis narrative. Bright core-collapse supernovae should emit a strong ^{44}Ti nuclear-decay signature, but observers have only detected ^{44}Ti radiation in dimmer supernovae (The *et al.* , 2006). Furthermore, the total ^{44}Ti detected in the sky is much less than the amount predicted by theoretical models (The *et al.* , 2006). Titanium is an important element for probing the anatomy of the supernovae, for it's production is very sensitive to its physical surroundings. Precisely because Titanium is so important in relation to understanding the environments inside SNe, these observational inconsistencies might have large theoretical implications.

Our research group, the Quark Nova Project, believes that these inconsistencies in the explosive nucleosynthesis model are not necessarily simple details that need to be fleshed

out in an otherwise, fundamentally correct model. We believe that the issues at-stake are paradigmatic in nature. We believe that perhaps, another mechanism needs to be suggested.

Perhaps this different mechanism lies in an alternate, "evolutionary channel" at the end of a star's life - the Quark Nova (QN). The Quark Nova (Ouyed *et al.* , 2002) is the explosive phase transition of a spin-down neutron star into a quark star. After a core-collapse supernova, the neutron star detonates and releases its neutron-dense layers, leaving behind a star made of entirely strange quark-matter. The environment in a QN is very adequate for various nucleosynthesis processes, which could fill in the gaps of the conventional theories. Past papers have explored the QN as a prime environment for the r-process (Jaikumar *et al.* , 2007; Ouyed *et al.* , 2009c).

My work is focused on an alternate nuclear process that happens in the QN - nuclear spallation. When the neutron star detonates, its neutron-dense and iron-rich ejecta collides against the ejecta of the prior cc-SN explosion, forming an interaction that was hereby called the dual-shock Quark Nova (dsQN). In this interaction, the neutrons and heavy isotopes that form part of the QN's ejecta, collide against the heavy isotopes in the cc-SN's ejecta, creating nuclear reactions. I believe this spallation nucleosynthesis might aid in solving some of the issues behind the r-process and Titanium production.

This spallation nucleosynthesis is the first of its kind. Before, nuclear spallation was merely used in the context of cosmic ray propagation. However, spallation nucleosynthesis is much more extensive than cosmic ray spallation - it's in a sense, a paradigm shift. It's a new angle for approaching the production of heavy elements. While most processes for the production of heavy elements depend on particle accretion - that is, a process where smaller nuclei and particles merge together to form larger daughter isotopes, spallation relies on fragmentation - where larger nuclei are broken into smaller, daughter isotopes.

This introductory chapter is meant to introduce the theoretical and observational context of spallation nucleosynthesis, so that papers presented in chapter two and three are

understood in their appropriate context.

1.1 Riddles in Conventional Theories of Explosive Nucleosynthesis

1.1.1 The Strange Case of ^{44}Ti Production

^{44}Ti is an isotope of importance in astrophysics. In conventional models, ^{44}Ti is produced in a stage of the cc-SN called the alpha freeze-out. The alpha-freeze occurs when the SN's shockwave passes through the Si-enriched layer of the star. The shockwave heats up and fragments the layer's nuclei into free α particles. The material eventually cools down and expands, which reassembles the α particles into heavier isotopes like ^{44}Ti (Jordan *et al.* , 2003).

This production of ^{44}Ti has serious observational and theoretical implications. First, it is one of the most observable probes that exist to tap the physical anatomy of cc-SNe. ^{44}Ca is the second most abundant calcium isotope, and the 44th most abundant specie in the solar system - where ^{44}Ca is a radioactive daughter isotope of ^{44}Ti (Clayton *et al.* , 1998). Furthermore, the late-time light curve of cc-SNe is powered by ^{44}Ti, which has led to indirect detection of ^{44}Ti by extrapolation from light curves (Woosley & Hoffman, 1991). This extrapolation is done by modelling the amount of luminosity emitted by radioactive ^{44}Ti. Moreover, ^{44}Ti 's half-life of ~ 60 years (Görres *et al.* , 1998) is long enough to let ^{44}Ti's decay γ-photons leave when the supernova's ejecta becomes transparent - as witnessed in the detection of γ-radiation in Cassiopeia A (Vink *et al.* , 2001) and recently SN1987A (Grebenev *et al.* , 2012). Finally, astronomers have identified ^{44}Ca in pre-solar grains (Clayton, 1971), which are believed to have condensed in the first few years after a cc-SN detonation when ^{44}Ti had not decayed fully. These grains might shed some light on the dynamics of SNe ejecta (Clayton, 1971).

Not only is ^{44}Ti a fairly visible probe, but it also has major consequences in cc-SN modelling. ^{44}Ti is produced near a region called the mass-cut. The mass-cut (Fig. 1.1) is

the geometrical border that separates the mass that will fall-back into the proto-neutron star from the mass that will be ejected outside of the proto-neutron star's gravitational potential. The mass-cut determines how much ^{44}Ti will fall into the proto-neutron star and therefore not be ejected - making the amount of ^{44}Ti ejected (and therefore detected) completely dependant to the location of the mass-cut. This location of the mass-cut is a key parameter that constraints the cc-SNe simulations (Clayton *et al.* , 1998). Moreover, the production of ^{44}Ti and ^{56}Ni is co-dependant because both of them are produced in the same region, making ^{44}Ti/^{56}Ni more or less constant. This co-dependence is important because ^{56}Ni is the main source of power of the cc-SN's light curve - which makes it of great astrophysical importance. Finally, production of ^{44}Ti is very sensitive to density, temperature, and Y_e [1], which makes the detection of ^{44}Ti key for modelling the environment in cc-SNe.

Unfortunately, the observations of ^{44}Ti are not quite congruent with the current models of cc-SNe. First, the amount of γ-radiation point-sources for ^{44}Ti currently detected is less than the amount expected from simulations (The *et al.* , 2006). Moreover, the ratio of ^{56}Ni/^{44}Ti detected in these point sources is less than the expected from models - in short, ^{44}Ti is overproduced at observed sites (The *et al.* , 2006). Finally, the most luminous cc-SNe, which in consequence have the most abundant ^{56}Ni, show no signs of ^{44}Ti - which contradicts the supposed co-dependwnce of both isotopes (The *et al.* , 2006).

Astronomers have suggested some explanations for some of these incongruencies. Nagataki *et al.* (1998) argued that the small ^{56}Ni/^{44}Ti ratio in observed sites is caused by asymmetric supernovae - which enhance ^{44}Ti at their explosion poles. This argument might explain the underproduction of ^{44}Ti by most cc-SN models - which are spherically symmetric. Magkotsios *et al.* (2010) explored ^{44}Ti for different parameters and thermodynamic trajectories and concluded that the scarcity of ^{44}Ti might be explained by its sensitivity to different profiles (e.g, different densities, electron fractions, and temperatures). Finally, The

[1] Y_e is the electron fraction, which is equivalent to the net number of electrons per baryon. A high Y_e implies a high proton to neutron ratio, for the total matter has to satisfy charge neutrality.

et al. (2006) argued that perhaps ^{44}Ti production is exceptional, and not a staple of a robust cc-SN model as previously expected.

However, these sketched solutions only tackle the issues in a piecemeal fashion. While asymmetric supernovae might explain the excess of ^{44}Ti at their observed sites, they do not explain the lack of detected point sources of ^{44}Ti radiation in the sky. Furthermore, the fact that Magkotsios *et al.* (2010) explain the paucity of ^{44}Ti as related to the sensitivity of ^{44}Ti to different thermodynamics and parameterizations is worrisome: Magkotsios *et al.* (2010) call implicitly into question the robustness of the cc-SN model in general.

Nonetheless, we believe that The *et al.* (2006) point in the correct direction - ^{44}Ti producing sites might be exceptional, and therefore demand a different nucleosynthetic model.

1.1.2 The Riddle of the r-process

The big bang created most of the hydrogen and helium in the Universe. Gravity accretes these light elements into massive bodies called stars. The stars compress these light elements into heavier elements through a nuclear reaction called fusion. These fusion reactions are exothermic, and release an outward, heat pressure that supports the star. However, these exothermic, fusion reactions cannot form elements heavier than ^{56}Fe. ^{56}Fe is the most tightly bound nucleus, and as such, the fusion into elements heavier than ^{56}Fe is endothermic - that is, the fusion reaction absorbs energy rather than release it. Furthermore, at these high Z numbers, the Coulomb interaction makes it impossible to form heavier elements by means of charged particles at these stellar temperatures. At this point, heavier isotopes can only be formed by neutron capture processes (Cowan & Thielemann, 2004).

The two major neutron capture processes are the slow neutron capture (s-process), and the rapid neutron capture (r-process). The s-process has a longer timescale for neutron capture than the time it takes for a neutron to β-decay into a proton, therefore, isotopes produced through this process stay close to the bottom of the valley of stability. In contrast, the r-process has a shorter timescale for neutron capture than the timescale for β-decay,

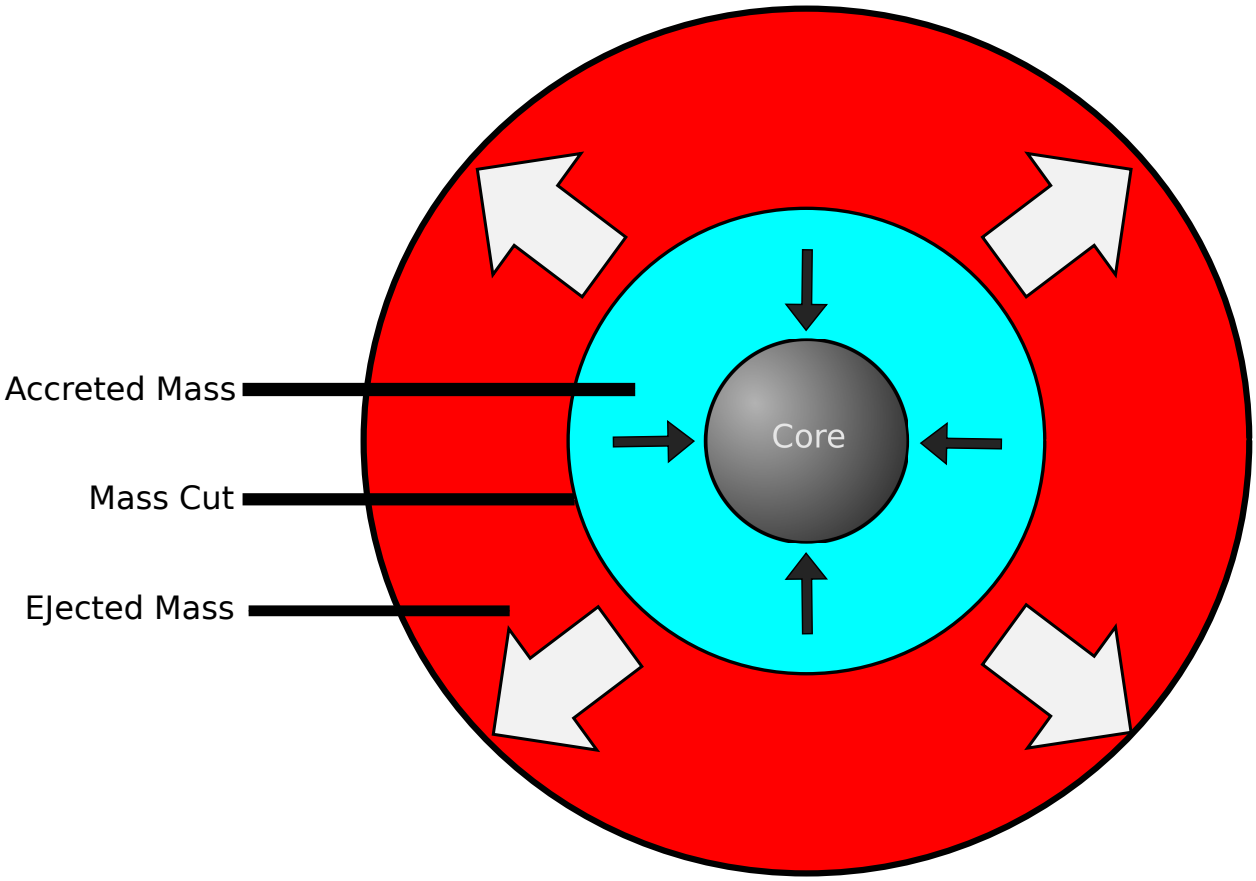

Figure 1.1: Diagram of a core-collapse supernova. The mass near the core is accreted and will consequently become part of the neutron-star/black-hole. The mass-cut is what separates the mass that will be ejected and the mass that will be accreted by the core. Ni and Ti are produced near the mass-cut.

therefore r-process elements can get closer to the neutron drip-line [2]. This means that the r-process can create heavier isotopes than the s-process by creating neutron-rich, unstable nuclei. Astronomers believe that the bulk of isotopes in the $56 < A < 90$ atomic mass range, are created through the s-process, while the r-process synthesizes most $A > 90$ isotopes (Cowan & Thielemann, 2004). The fusion inside stars and the neutron-capture processes are particle accretion mechanisms - that is, they synthesize daughter nuclei through the merger of smaller nuclei into larger nuclei.

Astronomers more or less agree that the astrophysical site for the s-process is the Asymptotic Giant Branch (Käppeler *et al.* , 2011)- a stage in the late-lives of all low- to intermediate-mass stars ($0.6 - 10$ $M_{\odot}$). However, the consensus surrounding the site for the r-process is much more ambiguous (Arnould & Goriely, 2012).

The density of neutrons necessary to trigger the r-process points to explosive sites. Historically, the cc-SN has been the prime candidate for this site. Early studies (Burbidge *et al.* , 1957) suggested that the neutron-rich flux ejected near the collapsing core in a supernova might be a prime environment for the r-process. However, soon this model encountered problems. For one, current simulations are only able to detonate under-powered explosions in intermediate-range mass ($8 - 15$ $M_{\odot}$) supernovae, and under very limited conditions (Burrows, 2013). In addition, even if the supernova is detonated artificially, the simulation is unable to recreate the right physical environment for the r-process (Arnould & Goriely, 2012). In order to trigger the r-process, the site should either contain a really high neutron/proton ratio, or manage with a lower neutron/proton ratio through a high amount of entropy (Arnould & Goriely, 2012). Researchers hoped that the neutrino winds emitted from the collapsing core, could raise the entropy sufficiently to trigger the r-process and therefore fix the problem. However, current simulations of neutrino winds in cc-SNe have been unable to recreate the large amount of entropy necessary (Roberts *et al.* , 2010)

[2]The neutron drip-line is the line in a nuclide chart that delineates the limit for the highest amount of neutrons per isotope. Its location is currently unknown.

Modellers have suggested other r-process candidates. Perhaps, Neutron Star Mergers (NSMs) are the second most discussed candidates. The decompressing, cold, neutron matter in the surrounding ejecta of the NSM has a sufficiently high neutron/proton ratio to trigger the r-process. The most glaring issue of the NSM is that they occur too late in the universe's lifespan. Studies have shown that old stars in the galactic halo exhibit r-process signatures, which imply that the r-process occurs early in the universe(Arnould & Goriely, 2012)- which contradicts NSMs' late coalescence. Moreover, NSMs underproduce isotopes of mass number $A < 120$, in comparison to solar abundances (Korobkin *et al.* , 2012).

In short, conventional models cannot offer a congruent site for the r-process. Not unlike the case of ^{44}Ti, perhaps an alternate or additional model is necessary.

1.1.3 The Quark Nova as the Missing Piece

Asymptotic freedom is the hypothesis that the interaction between quarks weakens as the space between them decreases. This hypothesis led to the conclusion that sufficiently high densities and/or temperatures lead to the de-confinement of hadronic matter into free quarks - strange quark matter. Witten (1984) suggested that strange matter is the lowest energy state of matter, to the extent that it is of lower energy than ^{56}Fe, the tightest bound of nuclei. If strange matter is the lowest energy state, then its existence as a stable stage of matter in the universe is a possibility. Current heavy ion collision experiments have led to evidence of the existence of Quark Gluon Plasma (QGP) - a form of hot, strange matter. (Aad *et al.* , 2010). Theorists have argued that the early, hot and dense universe was a QGP soup, and that the dense cores of compact objects might contain strange matter as well. Researchers have also suggested the existence a quark star, a compact object made of entirely strange matter (Weber, 2005).

What is the astrophysical phenomenology for the transition between hadronic matter and quark matter? Ouyed *et al.* (2002) argued that this phase transition in a spherical symmetry might lead to a core-bounce, which releases an energetic explosion. This highly explosive

phase transition was termed the Quark-Nova (QN). Furthermore, Niebergal *et al.* (2010) showed that the conversion front of neutrons into quarks within a highly dense neutron star leads to instabilities that detonate. In the wider picture of stellar physics, the QN acts as a new evolutionary channel for neutron stars in the $1.2 - 1.8$ $M_{\odot}$ range. If a neutron-star is in a spin-down evolution [3], as it slows down, the centrifugal force within it dissipates, increasing the central density of the neutron-star (Staff *et al.* , 2006). A sufficiently high central density then triggers the explosive, QN transition, expelling the neutron-crust and leaving behind a bare Quark Star (QS). Although direct evidence for the QN's existence is lacking, our group has proposed a large amount of indirect evidence (Leahy & Ouyed, 2008; Kostka *et al.* , 2012).

The QN is more than an interesting high-energy physics phenomenon. Although it contains cutting-edge physics, it also contains very important phenomenological consequences in astrophysics. The QN has been proposed as a model for Gamma Ray Bursts (Ouyed *et al.* , 2009b), Anomalous X-ray Pulsars and Soft Gamma-ray Repeaters (Niebergal, 2007), Ultra High Energy Cosmic Rays (Ouyed *et al.* , 2005b), and super-luminous supernovae (Leahy & Ouyed, 2008; Kostka *et al.* , 2012). Furthermore, the QN is an excellent site for nucleosynthetic processes, which include the r-process (Jaikumar *et al.* , 2007), and nuclear spallation reactions (Ouyed *et al.* , 2011). It is these nucleosynthetic processes - in particular nuclear spallation reactions - that are the focus of my work.

The QN as a site for nucleosynthesis might be the skeleton-key that unlocks the mystery of ^{44}Ti and the r-process. Jaikumar *et al.* (2007) presented the QN's neutron-rich ejecta as a hot and dense site for r-process reactions (Fig. 1.2). The site has the advantage of avoiding the neutron/entropy deficiency of standard cc-SNe models. Furthermore, QN can occur early in the universe, in contrast to NSMs, so QNe can cause the r-process enrichment observed in early stars (Ouyed, 2013; Ouyed *et al.* , 2009c). However, this QN model underproduces

[3]Spin-down evolution is the slow down of a neutron star's. Astronomers hypothesize that such slow-down can happen through the torque exerted by the neutron star's magnetic field, or through the emission of gravitational waves (Staff *et al.* , 2012)

isotopes in the $A < 130$ range.

In (Ouyed *et al.* , 2011), we argued that the peculiar ^{44}Ti signature of sub-luminous Cassiopeia-A indicated that Cassiopeia A is actually a QN remnant. This explanation clarified Cassiopeia A's excessive ^{44} Ti/^{56}Ni ratio as a signature of nuclear-spallation reactions. Furthermore, this fact explained the rarity of ^{44}Ti production sites- for such production was constrained by the event-rate and the conditions of the QN.

I believe that this groundwork done on QN nucleosynthesis can be extended. First, the inclusion of mixing in the cc-SN layers can lead to ^{44}Ti production in SNe that are not as sub-luminous as Cassiopeia A, such as SN1987A. Moreover, the addition of spallation to the QN's r-process model can produce $A < 130$ abundances, in contrast to the old QN r-process model and the NSM.

My work focuses on this generalization of the nuclear-spallation nucleosynthesis into a more universal model. In section 1.2, I give a brief introduction to the physics of nuclear-spallation. In section 1.3, I explore the specific spallation model I used in the context of the Quark-Nova.

1.2 An Introduction to Nuclear Spallation Physics

1.2.1 Brief History and Applications

Not unlike other branches of nuclear physics, nuclear spallation studies originated in astrophysics. In 1912-1913, Hess discovered the first cosmic rays in his balloon flights. These particle showers that fell from the sky, were a product of outer space, energetic particles. These outer space particles propagated through the earth's atmosphere through a chain of nuclear reactions - that is, through nuclear spallation reactions. The spallation products were the particles that Hess detected (Filges & Goldenbaum, 2010).

What constitutes nuclear spallation reactions is not clearly defined. Most definitions boil down to an energetic and relativistic, non-elastic collision, between two particles that

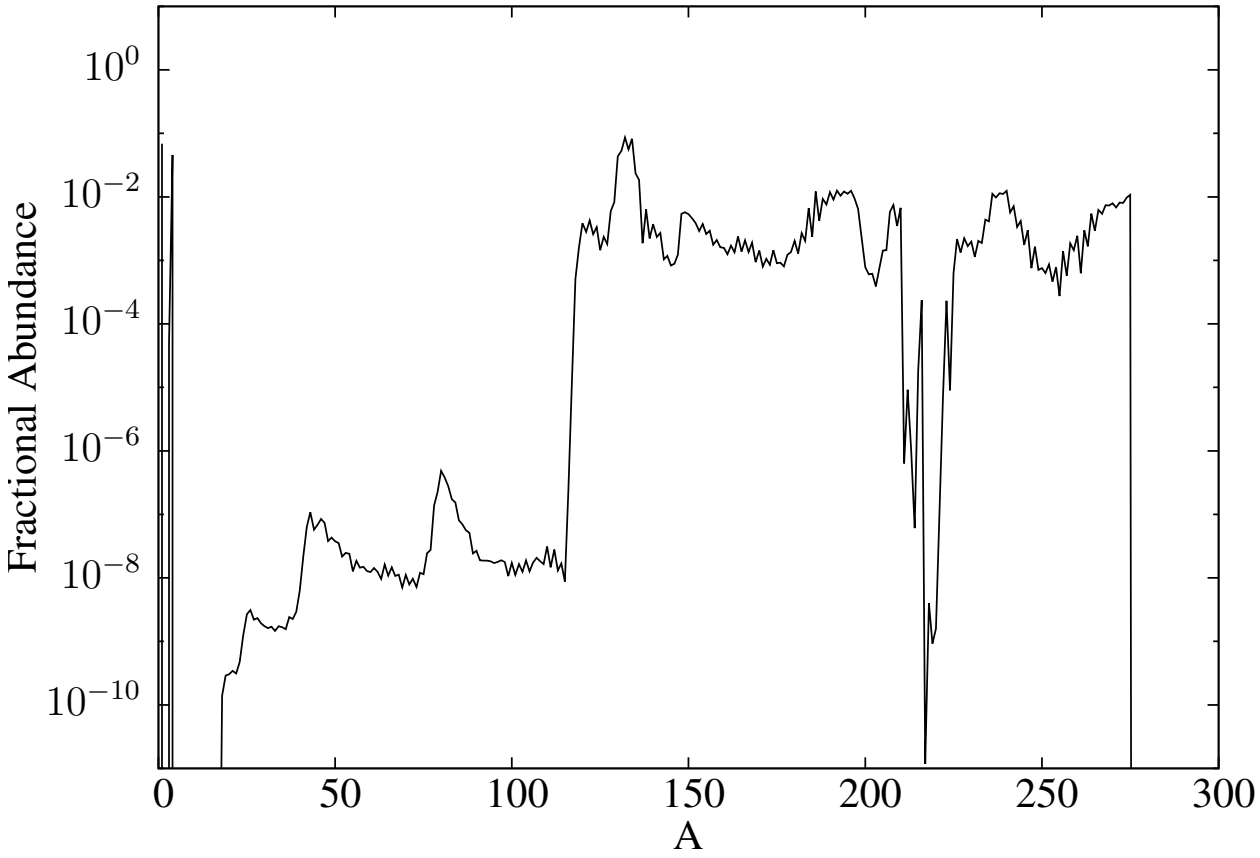

Figure 1.2: Abundance fractions produced in the QN ejecta, as a function of A. The abundances are produced through the r-process mechanism. This QN model produces an excess of heavy element but underproduces $A < 130$.

fragment into numerous, secondary particles (Filges & Goldenbaum, 2010). What energetic means depends on the context and is not an exact boundary. For proton-nucleus spallation reactions, the energy threshold for a proton projectile is about $\sim$ 100 MeV. (Filges & Goldenbaum, 2010)

In high-energy physics, nuclear spallation reactions are in the cutting edge, usually under the name of heavy ion collisions. Heavy isotopes, such as lead or gold, are accelerated at very high energies and then collided against each other. The collision generates extremely high temperatures and densities - making it a prime site for the study of exotic phase transitions. The QGP is one of these exotic phase states. The experiments at the Large Hadron Collider are perhaps the most well known examples of heavy-ion collisions.

In nuclear physics, heavy ion-collisions are used to synthesize rare isotopes. A beam of heavy isotopes is accelerated against a target, which fragments the beam into small fragments. These fragments can be neutron-rich and unstable, which gives an opportunity to study the behavior of nuclei near the neutron drip-line. The study of neutron-rich isotopes is important to understand the r-process better. (Schatz, 2008)

Spallation reactions are also used to create neutron sources. These neutron sources have their uses in the transmutation of nuclear waste, medical radiation therapy, and nuclear weapons (Krása, 2010).

In astrophysics, nuclear spallation reactions are mostly studied in the context of cosmic ray propagation. Cataclysmic events, such as supernovae, accelerate particles into high energies. These particles occasionally collide with inter-stellar gas as they propagate through space, generating spallation reactions. Furthermore, these particles, as they approach the earth, collide with the atmosphere's nuclei and generate spallation reactions. The particle showers generated by these spallation reactions are then detected by astronomers. In order to understand what where the primary sources of the detected showers, astronomers have to reconstruct the parent nuclei through spallation reaction simulations. (Filges & Goldenbaum,

Quark-Nova Reaction	Experiment
neutron-Ni spallation	Spallation Neutron Source (SNS)
nucleus-Ni spallation	Facility for Rare Isotope Beam (FRIB), and Large Hadron Collider (LHC)

Table 1.1: Some lab parallels to the spallation processes of the dsQN. The SNS is the most intense neutron pulse source in the world, which is produced by spallation between protons and liquid mercury (White *et al.* , 2002). The FRIB is a cutting edge facility, currently in development, for the production of rare-isotopes through the fragmentation of heavy nuclei spalled against a target (York *et al.* , 2009). In the LHC, heavy isotopes such as lead or gold are accelerated and collided against each other to produce exotic phase transitions (Andronic *et al.* , 2003).

2010). Finally, cosmic ray spallation is also the source of the so called cosmogenic nuclides [4], and specific isotopes of Be, B, and Li (Gosse & Phillips, 2001; Mashnik, 2000).

The dsQN model of spallation reactions is novel because it is the most extensive spallation-based nucleosynthesis process proposed in astrophysics. Although, cosmic rays have a fairly limited nucleosynthetic function, our QN model can produce ^{44}Ti and $90 > A > 130$ isotopes through spallation. The other nucleosynthesis models for heavy elements are based on particle accretion, where nuclei and small particles merge together to form heavier, daughter nuclei. However, spallation nucleosynthesis is based in the fragmentation of heavier nuclei into smaller particles - a process that is roughly the opposite of the more conventional, particle accretion models. Thus, the dsQN gives an astrophysical significance to physical processes that were mostly confined to cutting-edge labs (Table 1.1). I explore the specifics of this model in section 1.3.

[4]The cosmogenic nuclides are isotopes that are produced by the spallation of a cosmic ray particle against a solar system atom.

1.2.2 A Primer on Cross-Sections

Spallation reactions are complicated, and dynamic many-body problems. In order to simplify the problem, researchers have developed parameterized cross sections to calculate reaction yields.

A cross section is a quantity proportional to the probability for two particles to interact. A cross section has the dimensions of area, with the milibarn (mb) as its standard unit, where a barn = 10^{-24} cm^2. For pedagogical reasons, we can imagine a projectile i that passes through a slab of nuclei j. The cross section σ is defined such that the probability dP for a projectile i to interact with a nucleus j is,

$$dP = n \cdot \sigma \cdot dz \tag{1.1}$$

,

where n is the density of nuclei j and dz is the distance travelled by projectile i.

The total cross section between two particles is the sum of the elastic, and non-elastic interaction cross sections:

$$\sigma_{\text{total}} = \sigma_{\text{elastic}} + \sigma_{\text{non-elastic}} \tag{1.2}$$

The total, non-elastic interaction cross section is in turn, the sum of all the partial reaction cross sections:

$$\sigma_{\text{total inellastic}} = \sum_i \sigma_{\text{partial reaction,i}} \tag{1.3}$$

,

where i is summed across all partial reaction cross sections.

My dissertation makes ample use of cross-sections.

1.2.3 Proton-Nucleus and Neutron-Nucleus Reactions

Spallation is a high energy reaction, which implies that the projectile must have a large amount of kinetic energy. The kinetic energy of the projectile becomes much larger than the coulomb barrier, which makes the electromagnetic interaction between target and projectile immaterial. Thus, proton-nucleus and neutron-nucleus spallation reactions become interchangeable. For convention, I will generally refer to proton-nucleus spallation, but the underlying physics of neutron-nucleus reactions are very similar.

Proton-nucleus spallation can be roughly divided into two stages - the intra-nuclear cascade and de excitation.

The intra-nuclear cascade was first described by Serber (Serber, 1947). At energies of $\sim$ 100 MeV, a projectile proton's deBroglie's wavelength becomes comparable to the inter-nucleon distance of a nucleus (10^{-13} cm). This wavelength is small enough for the projectile to resolve individual nucleons inside a target nucleus, in contrast with resolving the whole nucleus. The projectile's collision with an individual nucleon transfers kinetic energy inside the target nucleus and causes an internal cascade of individual nucleon-nucleon reactions. At this stage, individual nucleons or fragments may acquire sufficient kinetic energy to escape the target as emissions. This stage leaves the target nucleus in an excited state. This stage is fairly short, with a $\sim 10^{-22}$ s timescale. (Krása, 2010)

The next stage is the de-excitation/evaporation phase. The excited nucleus will attempt to reach a lower energy level by releasing thermal particles isotropically. Some of these particles include neutrons, fragments, and γ-photons. After the end of the de-excitation phase, the resulting nucleus will usually undergo chain β decays until reaching a stable state. (Filges & Goldenbaum, 2010)

The total, non-elastic reaction cross-section for spallation between a proton and a nucleus can be parameterized geometrically. The proton projectile "sees" the nucleus as a circular target where the radius of the target is $\sim A^{2/3}$, and A is the mass number. A useful

parameterization for $E > 10$ MeV is (Letaw *et al.* , 1983),

$$\sigma_{\text{total}} = a \cdot A^{2/3} \text{ (mb)} \tag{1.4}$$

,

where $a \approx 50$ mb for A > 1.

In order to calculate the creation of product isotope with mass number A and atomic number Z, from a collision of a proton against target nucleus i, it's necessary to have a partial reaction cross section. Rudstam began the research on parametric, partial, reaction cross-sections for proton-nucleus reactions (Rudstam, 1966). His equation is,

$$\sigma_{\text{partial}} = \sigma_0 e^{-P\Delta A} e^{R|Z-SA+TA^2|^{3/2}} \tag{1.5}$$

where the factor $e^{-P\Delta A}$ describes the diminution of cross section as a function of the target-product mass number difference $\Delta A = A_i - A$. σ_0, P, R, S and T are adjustable parameters. The gaussian-like factor $e^{R|Z-SA+TA^2|^{3/2}}$ describes the statistical nature of de-excitation/evaporation. Most empirical partial reaction cross sections are modifications of the Rudstam equation.

1.2.4 Nucleus-Nucleus Reactions

Not unlike proton-nucleus spallation, the energy regimes for nucleus-nucleus spallation reactions are not exact. The energy range considered in this dissertation is about > 500 MeV/u (MeV/u means MeV per nucleon) per projectile. This energy is chosen because it's much larger than typical nuclear energy scales, like nucleon-separation energy and the Fermi energy that characterizes the nuclear ground state (Hüfner, 1985).

The frame of reference typically used is the projectile rest-frame but, the same physics apply in the target rest-frame as well. For brevity[s sake, I will only refer to the projectile rest-frame.

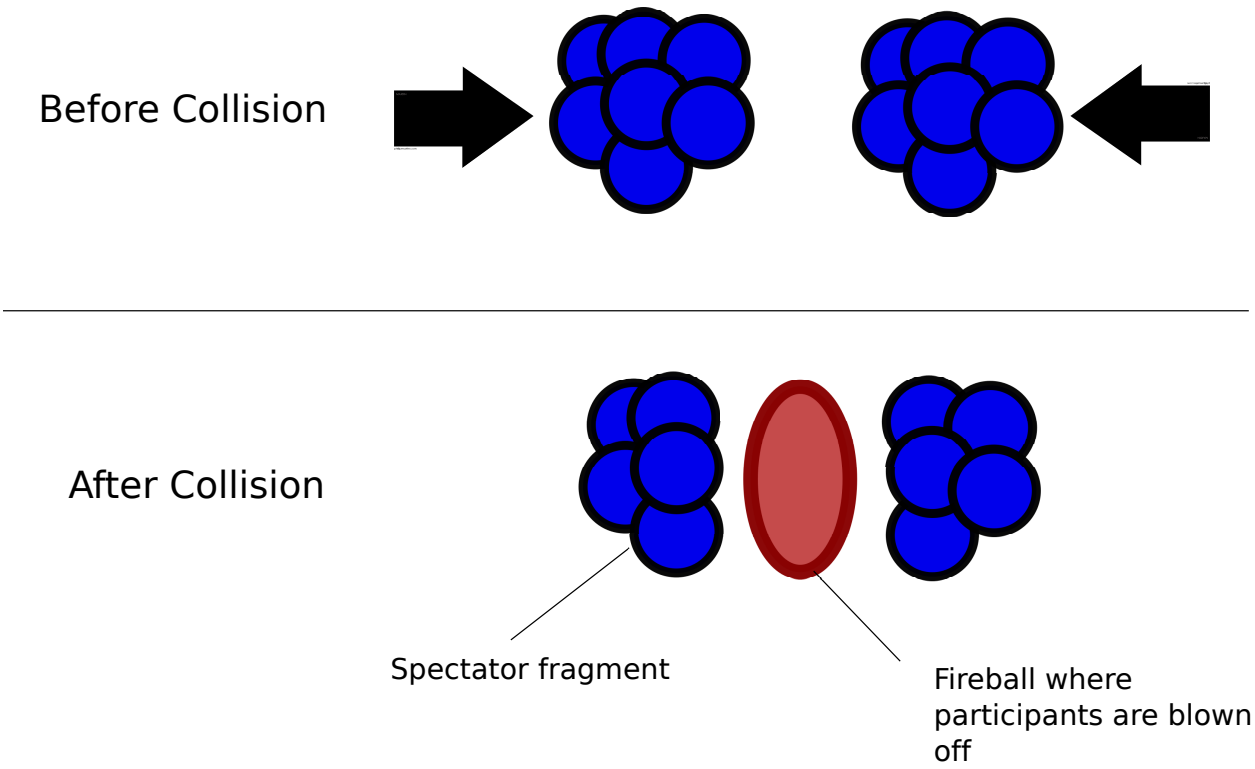

Figure 1.3: A collision between two nuclei. The hot nucleons blown off are participants, while the nucleons left behind are spectators. These spectator pre-fragments become the daughter nuclei created.

In nucleus-nucleus spallation reactions it is customary to divide the nucleons in the projectile and the target into participants and spectators. When two nuclei collide, the overlapping nucleons of the collision interact very intensely, creating a very hot and dense zone. These overlapping nucleons are called the participants. The cold, non-interacting nucleons are called the spectators. When two nuclei collide, the hot participant nuclei are blown off, leaving behind odd-shaped nuclei - pieces made of spectator nucleons. These pieces are unstable and are sometimes called pre-fragments (Fig. 1.3). The pre-fragments de-excite through the similar evaporation mechanism mentioned in 1.2.3. Usually, very little energy is lost in the collision, and therefore the projectile, spectator fragment continues in the same velocity as its pre-collision state, and the target fragment remains mostly static. These fragments are the daughter nuclei of the spallation reactions. (Hüfner, 1985)

The total reaction cross section can be parameterized geometrically following the idea behind (1.4)(Sihver *et al.* , 1993),

$$\sigma_{total} = \pi r_0^2 \left[A_p^{1/3} + A_t^{1/3} - b_0 \left[A_p^{-1/3} + A_t^{-1/3} \right] \right]^2, \tag{1.6}$$

$$b_0 = 1.581 - 0.876(A_p^{-1/3} + A_t^{-1/3}) \tag{1.7}$$

where, p is projectile, t is target, and $r_0 = 1.36$ fm. Where the b_0 is an overlapping parameter. This formula works for $E > 100$ MeV/u.

The partial reaction cross sections for nucleus-nucleus reactions can be scaled from the proton-nucleus reaction cross sections. The form of the equation is (Tsao *et al.* , 1993),

$$\sigma_{\text{partial,f}} = F(p,t) \cdot \sigma(p)_f \tag{1.8}$$

,

where $\sigma_{\text{partial,f}}$ is the cross-section for the production of fragment f from the collision of projectile p and target t. $\sigma(p)_f$ is the proton-nucleus reaction cross section for a proton

that collides against the projectile p in the projectile's rest-frame. $F(p,t)$ is a scaling factor that is a function of the proton and target and is calculated through an algorithm that uses Glauber scattering theory (Tsao *et al.* , 1993).

1.3 Our Spallation-Based Model

1.3.1 The Dual Shock Quark-Nova

The chronological evolution of a star into a dual-shock Quark-Nova (dsQN) begins with the evolution of a star into a core-collapse supernova. This explosion leaves behind a massive neutron-star. If the neutron-star undergoes a spin-down evolution, the centrifugal forces weaken and lead to a highly dense central-core. Another mechanism for increase in the core density is from fall-back material during the SN explosion or accretion (Ouyed & Staff, 2013). When the core reaches a critical density, quark de-confinement is triggered and propagates through a conversion front. The neutron-quark conversion front wrinkles and experiences instabilities, leading to the detonation of the neutron-star. The neutron star can also detonate through core-bounce (Ouyed *et al.* , 2002). This detonation releases a highly relativistic neutron-rich ejecta, leaving behind a bare Quark Star. If the time-delay $t_{\rm delay}$ between the prior cc-SN explosion and this neutron star detonation is large, then the cc-SN ejecta dissipates and the QN explodes in isolation. However, if this time-delay is only a matter of days or weeks, the relativistic, QN ejecta interacts with the inner layers of the cc-SN. This interaction is termed the dsQN (Fig. 1.4) (Leahy & Ouyed, 2008).

The dsQN was first explored as a model for the super-luminous supernova SN2006gy (Leahy & Ouyed, 2008). Super-luminous supernovae are more than 100 times more luminous than standard supernovae, and conventional models are unable to explain such high degrees of luminosity. However, the collision of the QN with the inner, cc-SN can reenergize the cc-SN ejecta. This collision can emit sufficiently high degrees of luminosity. The dsQN has led to encouraging light-curve fits for other super-luminous supernova as well (Leahy &

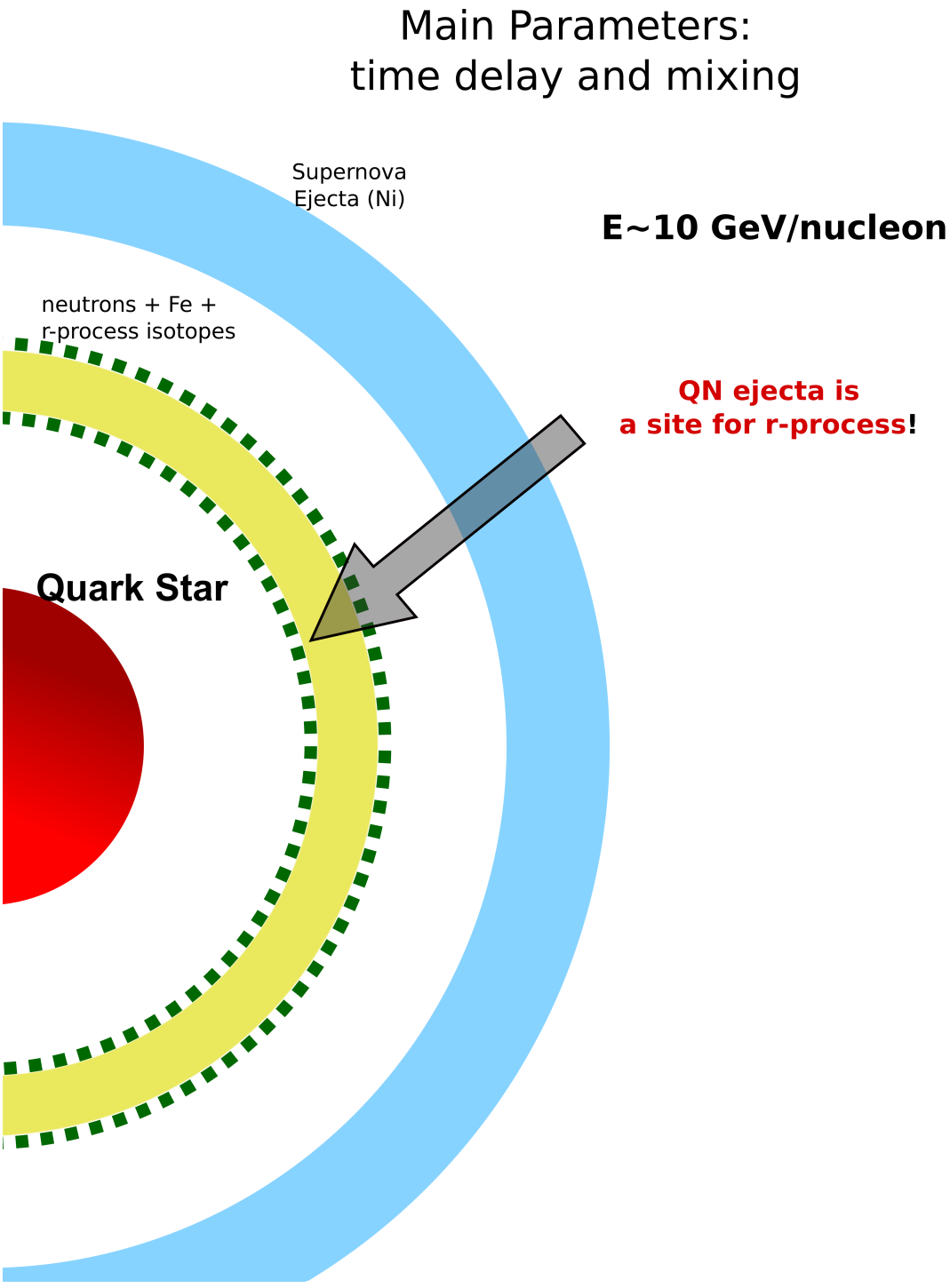

Figure 1.4: Diagram of the dsQN. The QN ejecta is rich with neutrons, Fe-peak elements, and r-process isotopes. The QN ejecta is expanding at a much faster speed than the SN ejecta, and thus, they will eventually collide against each other, and generate both neutron-nucleus and nucleus-nucleus spallation reactions.

Ouyed, 2008; Ouyed *et al.* , 2009a; Kostka *et al.* , 2012). The time delays considered for the super-luminous SNe are in the range of days $< t_{\rm delay} <$weeks.

Recently, the dsQN has been explored as an interesting model for spallation-based nucleosynthesis (Ouyed *et al.* , 2011). After the neutron star's detonation, the QN ejecta's neutrons and heavy isotopes can spall against the isotopes of the cc-SN's inner layers. These spallation-reactions are triggered at a $t_{\rm delay}$ in the order of a few days, when the SN's layers are sufficiently dense. Furthermore, the low $t_{\rm delay}$ causes the dense SN ejecta to consume the imparted QN energy as PdV work, which avoids super-luminosity. These spallation-reactions create a fairly extensive, nucleosynthetic mechanism.

1.3.2 Dual-Shock Quark Nova and Neutron-Nucleus Reactions

Our group first explored the spallation physics of the dsQN in the context of Cassiopeia A (Ouyed *et al.* , 2011). The supernova-remnant of Cassiopeia A is a strange scenario. γ-ray telescopes detected a large ^{44}Ti mass in Cassiopeia A, which would indicate a large abundance of ^{56}Ni in the context of conventional, cc-SN models. However, the observations made by Flamsteed imply that CasA was probably not a very bright cc-SN. This low luminosity would imply that the cc-SN did not produce a high amount of ^{56}Ni. Thus, the observations indicate that Cassiopeia A was a ^{56}Ni deficient, but with abundant ^{44}Ti. As mentioned in section 1.1.1, a high ^{44}Ti/^{56}Ni ratio does not bode well theoretically. In addition, Ouyed *et al.* (2011) showed that the amount of point-sources of ^{44}Ti detected in the sky was less than what was theoretically expected. In that paper, Cassiopeia A was postulated a an exceptional event.

Not unlike The *et al.* (2006), we also argued that Cassiopeia A was a unique event. However, in contrast to The *et al.* (2006), we offered a physical explanation for the peculiarities of Cassiopeia A - the supernova remnant is actually the remnant of a dsQN (Ouyed *et al.* , 2011).

We explained the peculiarities of Cassiopeia A in the following way. The neutrons released

in the QN explosion collide against the inner, Ni-layer of the prior cc-SN explosion, creating spallation reactions. These reactions destroy a large amount of Ni and synthesize a large amount of Ti - creating the abnormally high ^{44}Ti/^{56}Ni ratio. The rarity of point-sources of ^{44}Ti is of direct consequence to the constraints set up by the dsQN scenario. The dsQN is constrained by the QN event rate, and the specific $t_{\rm delay}$ range necessary for the production of abundant ^{44}Ti (Ouyed *et al.* , 2011) . If ^{44}Ti is not a signature of conventional cc-SNe, but of the dsQN, then this fact would explain the excess of Ti point sources predicted by conventional models.

Paper 1 is an extension of the Cassiopeia A model. In (Ouyed *et al.* , 2011), the dsQN was specifically tailored for Cassiopeia A, that is, to create a Ni-deficient but Ti-rich object. However, we universalize this dsQN neutron-nucleus spallation model and make it more robust by considering mixing in the cc-SNe layers. Mixed SN layers would send Ni bullets into the outer layers, which leaves less Ni to be destroyed by spallation neutrons. However, spallation reactions can still create abundant Ti from the smaller amount of Ni left behind. We explore this model more extensively in Paper 1 and in section 3.2.

1.3.3 Dual Shock Quark Nova and Nucleus-Nucleus Reactions

As explained in section 1.1.2 and 1.1.3, current candidate sites for the r-process fail to explain the solar abundances of $A > 90$ isotopes. Even the QN model as it stands is not completely satisfactory, because it underproduces $A < 130$ elements. In Paper 2, we correct the the old, QN r-process model, by extending it into the dsQN picture. In the dsQN picture, the r-process ejecta collides against the prior cc-SN ejecta, generating nucleus-nucleus spallation reactions. This spallation reactions enhance the $A < 130$ isotopes, bridging the $90 > A > 130$ gap of the old, QN model. Thus, the dsQN becomes the site for a universal, nucleus-nucleus spallation nucleosynthetic mechanism. We explore this model more extensively in Paper 2 and in section 3.2.

1.3.4 The Model and the Papers

The model that we use in Paper 1 and Paper 2 is an extension of the spallation model that was applied to the peculiar case of Cassiopeia A (Ouyed *et al.* , 2011). For pedagogical reasons, we visualize the dsQN as a particle-accelerator lab experiment. Using the terminology of accelerator physics, we divide the model into a beam and a target. We also add "collision statistics" as a further category.

- Beam: The QN ejecta is interpreted as the beam. Studies have shown that the QN can eject $\sim 10^{-3}\mathrm{M}_{\odot}$ of neutron rich-matter (Keränen *et al.* , 2005; Ouyed *et al.* , 2005a). In Paper 1, we model the beam as a pulse of $N_0 = 4.2 \times 10^{54}$ neutrons with a relativistic energy of 10 GeV. This neutron-beam is used to explore neutron-nucleus and proton-nucleus spallation in the context of the dsQN. In Paper 2, we model the beam as a pulse of $\sim 10^{-5}\mathrm{M}_{\odot}$ of ^{130} Ba nuclei, with an energy of $10GeV/u$. The ^{130}Ba nuclei represents a typical r-process element in the dQN ejecta (Jaikumar *et al.* , 2007). The collision of the ^{130}Ba beam against the ^{56}Ni target will generate nucleus-nucleus spallation reactions.

- Target: The expanding, SN ejecta is interpreted as a target. We model the inner layers of the SN as the target. The target expands, spherically, with an outer radius of $R = v_{\mathrm{sn}} t_{\mathrm{delay}}$, where v_{sn} is the speed of the expanding ejecta. The target has a constant density of $n = N/(4\pi R^2 \Delta R)$, where ΔR is the thickness of the target and N is the number of nuclei in the target. Paper 1 and Paper 2 further explain the specificities of this target.

- Collision Statistics: For simplicity, Paper 1 and Paper 2 divides the Target into radial, virtual layers (Fig. 1.5). In each layer, all particles of the beam collide simultaneously. The layers are separated by a mean free path $\lambda = 1/(n\sigma_{\mathrm{total}})$,

where σ_{total} is the total, non-elastic reaction cross section. Paper 1 and Paper 2 use different techniques to calculate the probability of creating a particular fragment. These techniques are explained in the papers.

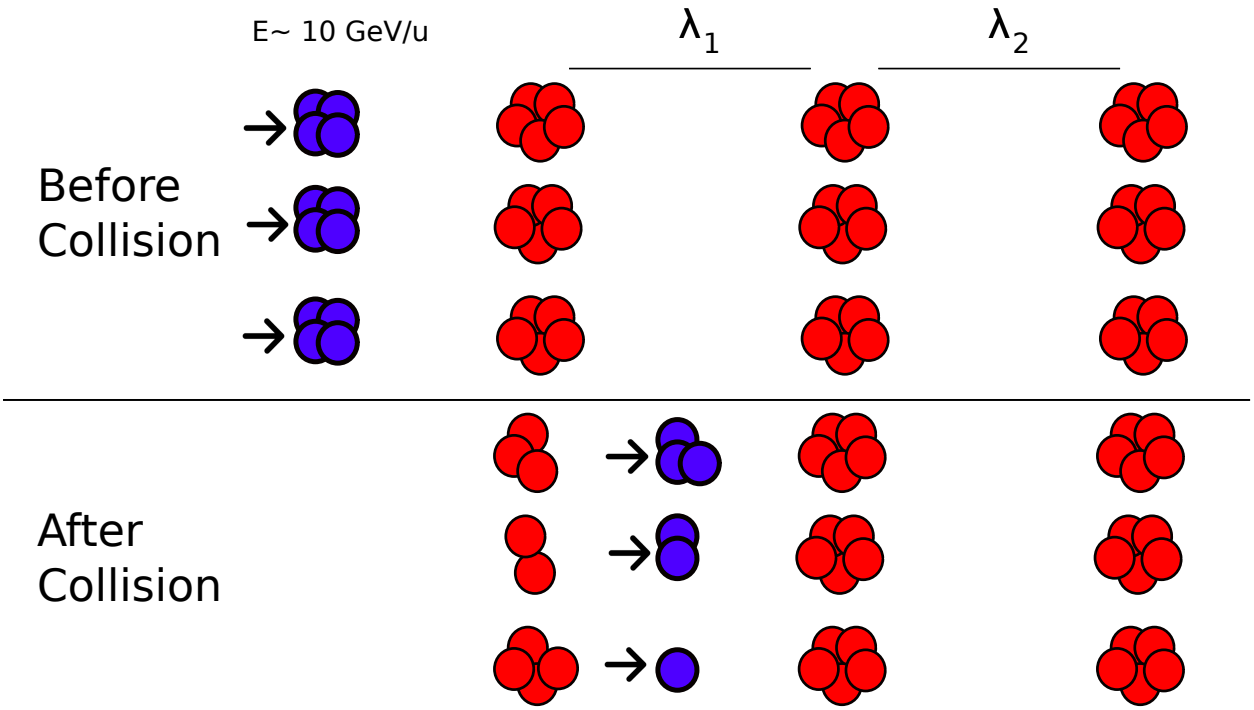

Figure 1.5: Diagram of the collision statistics. The red nuclei represent the target, and the blue nuclei represent the projectiles. The blue nuclei are divided into virtual layers separated by λ. This particular figure represents nucleus-nucleus collisions, where both the projectiles and the targets become fragmented.

1.3.5 My Contributions to Paper 1 and Paper 2

I wrote, almost entirely by myself, Paper 1 and Paper 2. Nonetheless, for both papers, I received extensive input from my advisors, Rachid Ouyed and Denis Leahy, both in matters of scientific content and editing. Prashanth Jaikumar was also a major source of input in Paper 1. Furthermore, the code used in Paper 1 was almost completely based in a code written by Rachid Ouyed and Denis Leahy (Ouyed *et al.* , 2011) - I simply added the appropriate modifications for mixing. For Paper 2, I wrote the code used to simulate nucleus-nucleus collisions in the dsQN. However, for the calculation of the empirical partial cross sections of proton-nucleus reactions, I used publicly available routines (Silberberg *et al.* , 1998).

Chapter 2

Paper 1

We wrote this paper to universalize the neutron-nucleus spallation model we first used for Cassiopeia A (Ouyed *et al.* , 2011). In Cassiopeia A, QN-ejecta neutrons destroy large amounts of ^{56}Ni through spallation reactions, giving Cassiopeia A its Ni-deficient, sub-luminous profile. These spallation reactions, in turn, create a large ^{44}Ti abundance. However, signatures in the bolometric light curve and γ-ray spectroscopy have shown that some non sub-luminous cc-SN-like objects should have a large, ^{44}Ti abundance as well. We therefore extend the dsQN model we used in Cassiopeia A to account for SN ejecta mixing. In addition, this paper explores the late-time light curve and γ-ray spectroscopy for the dsQN model using different mixing parameters. Finally, it offers a few, unique, astronomical signatures that would help in discriminating dsQN from other objects. This paper is important because it suggests that the theoretical issues faced by ^{44}Ti production could be solved if ^{44}Ti point-sources are considered a dsQN signature.

A Spallation Model for ^{44}Ti production in Core Collapse Supernovae

Amir Ouyed[1], Rachid Ouyed[1], Denis Leahy[1], and Prashanth Jaikumar[2]

Department of Physics and Astronomy, University of Calgary, 2500 University Drive NW, Calgary, Alberta, T2N 1N4 Canada[1]

Department of Physics and Astronomy, California State University Long Beach, 1250 Bellflower Blvd., Long Beach CA 90840 [2]

2.1 Introduction

Late time light curves of SNe are considered a relatively accessible resource for studying the nature of SNe, yet, the study of these light curves is ridden with challenges. Very few objects have been studied beyond $\sim$ 200 days, because as the SN dims out, the dust and the background noise, makes the signals unreadable (Leibundgut & Suntzeff, 2003). Even the most extensively documented supernova, SN1987A, is difficult to study at its later stages, because it is very hard to extrapolate directly the bolometric luminosity after $\sim$ 1400 days (Leibundgut & Suntzeff, 2003). The lack of late time light curve data make it difficult to formulate standard SN models. SN models have their parameters adjusted so that the isotopic yields reflect the abundances inferred from late time light curves (Limongi & Chieffi, 2006), which makes them dependent on the quality and understanding of our current observations. An example of the problematic nature of standard core collapse SN models, is ^{44}Ti production. Although ^{44}Ti production is assumed to be universal in cc-SNe models (The *et al.* , 2006; Woosley *et al.* , 1995), only SN1987A is documented well enough to be able to extrapolate ^{44}Ti from the bolometric light curve. The problem is precipitated by the fact that current telescopes have only been able to detect ^{44}Ti decay lines in Cassiopeia A (The *et al.* , 2006), and recently in SN1987A (Grebenev *et al.* , 2012), whereas current models predict more detections (The *et al.* , 2006).

In this paper, we attempt to solve some of these problems by proposing an alternative channel to the standard cc-SN model. After the SN explosion, neutron stars that undergo an evolution (e.g. matter fallback, or spin-down) towards quark deconfinement densities will transition to a lower energy, strange matter phase and experience an energetic detonation. (Quark Nova or QN) (Ouyed *et al.* , 2002). The neutron star will release its outer layers as relativistic, neutron rich ejecta (Keränen *et al.* , 2005; Ouyed *et al.* , 2005a; Niebergal *et al.* , 2010), where the ejecta interacts with the SN envelope (dual-shock Quark Nova, or dsQN). The time delay (hereafter $t_{\rm delay}$) between the two detonations constrains the nature of the interaction, where a time delay on the order of days will cause significant spallation of SN ejecta by QN neutrons. The spallation reaction creates unique signals in the late time light curve due to the modification of radioactive isotope abundances. The time delay $t_{\rm delay}$ between the QN and SN detonations acts as a parameter for the isotopic abundances. The different abundances of isotopes will also create specific γ spectroscopic signals. Currently, there have been many indirect observations for QN suggested (e.g. Hwang & Laming (2012); Ouyed *et al.* (2012); Leahy & Ouyed (2008); Ouyed (2013a); Ouyed & Leahy (2012)).

In continuation to Ouyed *et al.* (2011), we explain the ^{44}Ti synthesis measured in the late-time light curves of cc-SNe (Woosley & Hoffman, 1991) as a product of nuclear spallation from the dsQN, in contrast to the traditional view that it is produced by the SN in situ. The conditions necessary for the production of a QN, and the constraints set by the parameter $t_{\rm delay}$, explains the rarity of observations of ^{44}Ti nuclear decay lines. In contrast to our earlier paper (Ouyed *et al.* , 2011), we avoid excessive destruction of ^{56}Ni by spallation, by taking into account the mixing of the SN's layers. Current observations observations seem to support the picture of mixing (Mueller *et al.* , 1991). Furthermore, numerical studies have shown that Rayleigh Taylor instabilities can cause considerable mixing in a very short time span (Kifonidis *et al.* , 2000; Hachisu *et al.* , 1991; Mueller *et al.* , 1991). If ^{56}Ni is mixed through the SN envelope, there are less ^{56}Ni nuclei in the inner layer. This would lead to

QN neutrons hitting less ^{56}Ni, as opposed to the picture where all ^{56}Ni is concentrated in the inner layers (Ouyed *et al.* , 2011). By avoiding excessive nickel depletion, we can avoid the sub-luminosity characteristic in Ouyed *et al.* (2011).

2.2 Model

We extend the model we presented in Ouyed *et al.* (2011) by including mixing. In analogy to lab terminology, we divide our model into a beam part, and a target part. The scenario consists of a beam of relativistic QN ejecta that collides with a target that is the expanding, inner layers of the SN envelope. The time delay between the SN denotation and neutron star detonation and the mixing of the SN ejecta are the key parameters in our model.

2.2.1 Beam

In past studies (Keränen *et al.* , 2005; Ouyed *et al.* , 2005a; Niebergal *et al.* , 2010), the authors explored the explosion mechanism of the neutron star and the dynamics of the QN ejecta. A neutron star can detonate through an explosive conversion into a quark star and eject its outer most layers as a mass of $M_{QN} \sim 10^{-3}$ M$_\odot$. We can model the QN ejecta as a pulse of $N^0 \sim 1.2 \times 10^{54} M_{QN,-3}$ neutrons where $M_{QN,-3}$ means M_{QN} in units of 10^{-3} M$_\odot$. The neutrons are relativistic, with an energy of ~ 10 GeV (Ouyed *et al.* , 2011).

2.2.2 Target

We model the target as an expanding SN envelope of inner radius $R = v_{\rm SN} t_{\rm delay}$, where $v_{\rm SN} =$ 5000 km/s is the typical velocity of the SN ejecta, and $t_{\rm delay}$ is the time delay between the neutron star detonation and the SN detonation. We assume the exploding star is ~ 20 M$_\odot$. In contrast to the original model (Ouyed *et al.* , 2011), we assume different degrees of mixing. The target is the inner layers of the expanding SN envelope, which is composed of ^{16}O,^{12}C, and ^{56}Ni, whether these isotopes are stratified into separate layers or mixed. We assume

that whole SN envelope has a total ^{56}Ni mass of ~ 0.1 M$_\odot$, and O and C have total masses of ~ 1.0 M$_\odot$ each (Ouyed, 2013a). We treat a target, number density n as radially constant, where,

$$n = n_{\rm Ni} + n_{\rm O} + n_{\rm C} = \frac{N}{4\pi R^2 \Delta R}, \tag{2.1}$$

where ΔR is the thickness containing a layer and N is total number of nuclei within ΔR. Our mean free path λ is,

$$\lambda = \frac{1}{n_{\rm Ni}\sigma_{56} + n_{\rm C}\sigma_{12} + n_{\rm O}\sigma_{16}}, \tag{2.2}$$

where we use the semi-empirical cross section $\sigma_A = 45$ mb $\times A^{0.7}$ (Letaw *et al.* , 1983), where A is mass number. For our model, we use (2.1) and (2.2) to divide the thickness ΔR into $N_{\rm coll}$ imaginary layers of width λ,

$$N_{\rm coll} = \frac{\Delta R}{\lambda} \approx 57.54 \frac{\frac{M_{\rm Ni,0.1\ M_\odot}}{56^{0.3}} + \frac{M_{\rm O,0.1\ M_\odot}}{16^{0.3}} + \frac{M_{\rm C,0.1\ M_\odot}}{12^{0.3}}}{v_{SN,1000{\rm km/s}} \times t_{\rm\ delay,10\ days}}, \tag{2.3}$$

where $N_{\rm coll}$ represents the number of collisions an incoming neutron travelling within distance ΔR. The subscript indicates the units, for example, $M_{\rm O,0.1\ M_\odot}$ is in units of 0.1 M$_\odot$. The interaction of that neutron with a SN nucleus of mass number A will release a multiplicity ζ of nucleons,

$$\overline{\zeta}(E, A) \approx 4.67 A_{56}(1 + 0.38 {\rm ln} E) Y_{\rm np}, \tag{2.4}$$

where

$1.25 < Y_{\rm np} < 1.67$ (Cugnon *et al.* , 1997; Ouyed *et al.* , 2011).

2.2.3 Spallation Statistics

At each layer k of radial thickness λ, an nucleus will be bombarded by $N^0_{\rm hits}$ neutrons, resulting in the nucleus (Ouyed *et al.* , 2011),

$$A^1 = A^0 - \sum_{j=0}^{N^0_{\rm hits}-1} \zeta^0(E^0, A^j). \tag{2.5}$$

We represent the fraction of neutrons that hit a target of a particular element i as $w_i \sim N_i/N_{\text{total}} \sim M_i/(N_{\text{total}} A_i m_H)$, where N_i is the total number of nuclei of isotope i, M_i is the inner mass of a specific isotope i, m_H is the mass of a proton, and A_i is the atomic number of isotope i. The statistical weight signifies the fraction of nuclei of that particular element that will be hit by the incoming neutrons.

N^0_{hits} and ζ_0 are drawn from a Poisson distribution that peaks at,

$$\overline{N}^0_{\text{hits}} \sim \left(\frac{N_{\text{Ni}}\sigma_{\text{Ni}} + N_{\text{C}}\sigma_{\text{C}} + N_{\text{O}}\sigma_{\text{O}}}{N_{\text{Ni}} + N_{\text{C}} + N_{\text{O}}}\right)\left(\frac{N^0(1-e^{-1})}{4\pi R^2}\right), \tag{2.6}$$

where N_i is the number of nuclei of isotope i, and σ_i is the spallation cross section for isotope i.

For subsequent layers, it follows that.

$$\overline{N}^k_{\text{hits}} = (1-e^{-1})\overline{\zeta}^k \overline{N}^{k-1}_{\text{hits}} \tag{2.7}$$

and the mean nucleon energy for each subsequent layer is,

$$E^k \sim \frac{E^{k-1}}{\overline{\zeta}^{k-1}} \tag{2.8}$$

where spallation ceases at an energy of $E \sim 73$ MeV (Cugnon *et al.* , 1997).

2.2.4 Mixing

The isotope production in our model strongly depends on the nature of the mixing in the target. We therefore define mixing as a parameter, where an unmixed state, and a total mixed state form the two most extreme values of the parameter. Furthermore, we use a third "half-mixed" state, that lies between the two extremes. For simplicity, we assume that the angular distribution of each isotope specie is relatively homogenous in the inner layers, so equation (2.1) applies. In the model, the unmixed state follows an onion layer profile, where the target is stratified into layers where each layer is made of a specific isotope. In our case,

there is the innermost layer made of $M_{Ni} = 0.1$ $M_\odot$, followed by a second layer of $M_O = 1.0$ $M_\odot$, and a third layer of $M_C = 1.0$ $M_\odot$. The half-mixed state is still stratified into layers, but the ^{56}Ni layer is contaminated by O, and the O layer is contaminated by a small amount ^{56}Ni, and the C layer remains pristine. So, for the half-mixed state, the first layer consists of $M_{Ni} = 0.05$ $M_\odot$ and $M_O = 0.05$ $M_\odot$, the second layer of $M_{Ni} = 0.05$ $M_\odot$ and $M_O = 0.95$ $M_\odot$, and the third layer of $M_C = 1.0$ $M_\odot$. We define the total mixed state as a state where the mixing has spread the total mass of each of the original isotopes homogeneously through the entire envelope, effectively destroying layer stratification. The masses of an an inner, mixed 1.0 $M_\odot$ target then become $M_{Ni} = 0.0476$ $M_\odot$, and $M_O = M_C = 0.476$ $M_\odot$. In the case of the total mixed state, we treat the SN envelope as one layer with equation (2.1), where the layer contains the mixed ^{56}Ni,O and C.

2.2.5 Light Curve Model

We compute the late time light curve by extending our spallation code with the Supernova Light Curves' Code for Cococubed program (Timmes, n.d.). Our spallation code computes the mass yields of different isotopes using the model in Section 3.2, and the Cococubed extension computes the bolometric luminosity from the isotope mass yields. We also take into account the contributions of ^{57}Ni, and ^{60}Co to the bolometric light curve, and we take their mass values from Woosley *et al.* (1995). In our model, we assume the simple case where the bolometric luminosity is entirely caused by the thermalization of nuclear decay radiation.

2.3 Results

2.3.1 Photometry

The key isotopes for the light curve (Fig. 2.2) are ^{56}Ni and ^{44}Ti.

In Fig 2.1, we notice that the luminosity of the first $\sim$ 1000 days strongly depends on

mixing. This is because the amount of mixing dictates how much ^{56}Ni is available in the inner layers as target for QN neutrons. In the first $\sim$ 1000 days ^{56}Ni decay radiation dominates the bolometric luminosity. Mixing transports nickel into the outer shells, so if mixing increases, less nickel is available in the inner layers to be destroyed by energetic neutrons. An unmixed target experiences the most destruction of ^{56}Ni, which translates into a lower luminosity in the first days of the light curve. In Ouyed *et al.* (2011), we explored an unmixed dsQN as a possible candidate for Cassiopeia A. We argued that an unmixed dsQN was a plausible candidate because the sub-luminosity caused by ^{56}Ni depletion correlated with Flamsteed's sub-luminous observation, and the ^{44}Ti synthesis caused by ^{56}N spallation correlated with COMPTEL's and BEPPO SAX's ^{44}Ti detection (Iyudin *et al.* , 1994; Ouyed *et al.* , 2011).

We notice that the luminosity is less strongly affected by the mixing after $\sim$ 1000 days. This weaker dependance is due to the fact that ^{44}Ti synthesis does not seem to change as much across mixing space. Even if ^{44}Ti does vary across the different mixed states, the order of magnitude $M_{Ti} \sim 10^{-4}$ $M_\odot$ stays the same.

For $t_{delay} = 4$ days, and total mixing, our model synthesized $\sim 10^{-4}$ $M_\odot$ of ^{44}Ti, which compares favourably to amounts found by γ-ray telescopes in Cassiopeia A (Iyudin *et al.* , 1994), amounts estimated from the light curve of SN1987A (Suntzeff *et al.* , 1992; Woosley & Hoffman, 1991), and the amount detected with INTEGRAL (Grebenev *et al.* , 2012). Furthermore, we notice there is very little nickel that is depleted - indeed most of the original inner 0.0476 $M_\odot$ is maintained for 3 days $\leq t_{delay} \leq$ 10 days. If very little ^{56}Ni is depleted from the inner mass, then the total $\sim$ 0.1 $M_\odot$ for ^{56}Ni that is spread throughout the whole envelope, is more or less maintained throughout different time delays. The $\sim$ 0.1 $M_\odot$ mass for ^{56}Ni compares quite well with what is observed in type II SN light curves (Suntzeff *et al.* , 1992; Woosley & Hoffman, 1991). Another interesting isotope is ^{22}Na, and it is synthesized at a high amount of almost $\sim 10^{-4}$ $M_\odot$ which contrasts with the estimates of $\sim 10^{-6}$ $M_\odot$ (Woosley *et al.* , 1995). This creates a higher contribution to the bolometric luminosity, than

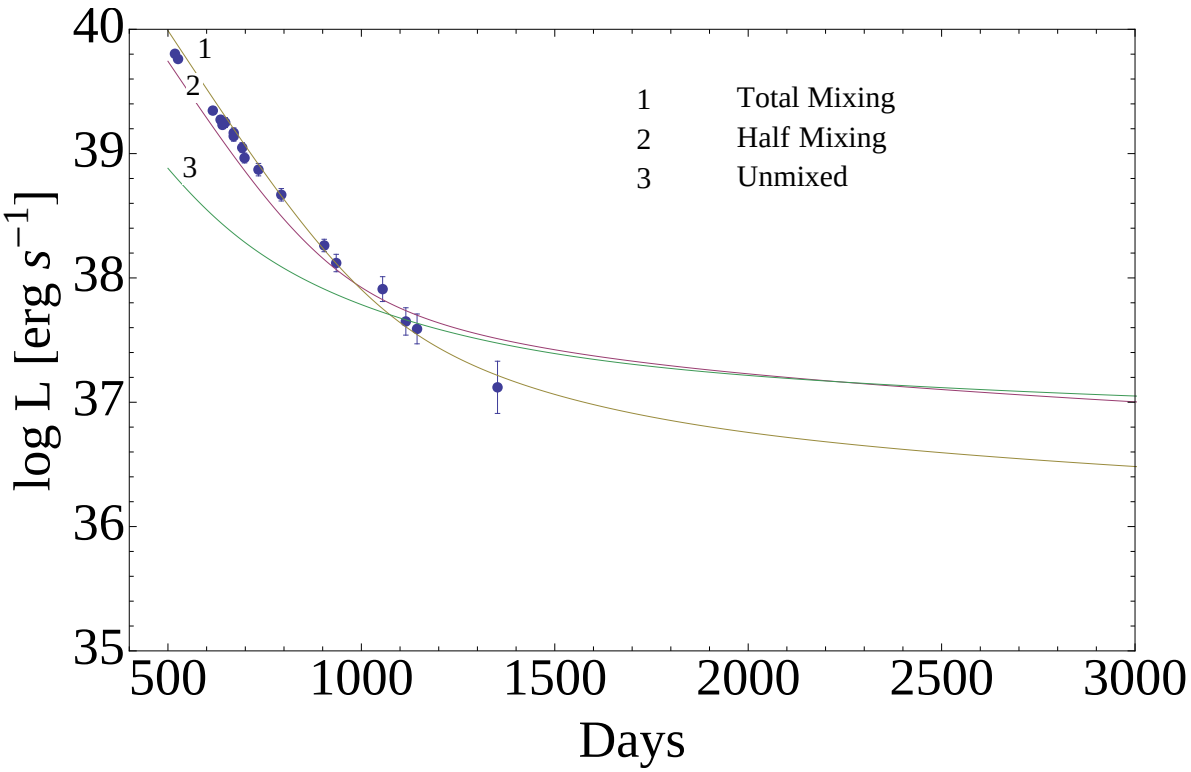

Figure 2.1: Light curves of our model at $t_{\rm delay} = 4$ days for different mixing states and the SN1987A data. The SN1987A data comes from Suntzeff *et al.* (1991) and is plotted for reference. The points are the SN 1987A data and the solid lines indicate our model. The y-axis is the logarithm of luminosity in units of erg/sec.

normally expected. We see in the upper panel of Fig 2.2 a dependance of the light curve to $t_{\rm delay}$. We can see that latter stages of the late time light curve are the most visibly affected by the time delay. This strong dependance in the later days is modulated by the production of ^{44}Ti, because ^{44}Ti yields are very affected by the time delay (Fig. 2.4). The earlier days of the late time light curve seem to be affected only weakly by the time delay change, because ^{56}Ni destruction stays more or less constant (Fig. 2.4). This weak dependance of ^{56}Ni to $t_{\rm delay}$, at least for the total mixed state, is interesting because ^{56}Ni varies a lot across mixing space. In contrast, we find that for the total mixed state, ^{44}Ti production depends strongly on $t_{\rm delay}$. but it varies very weakly across mixing space.

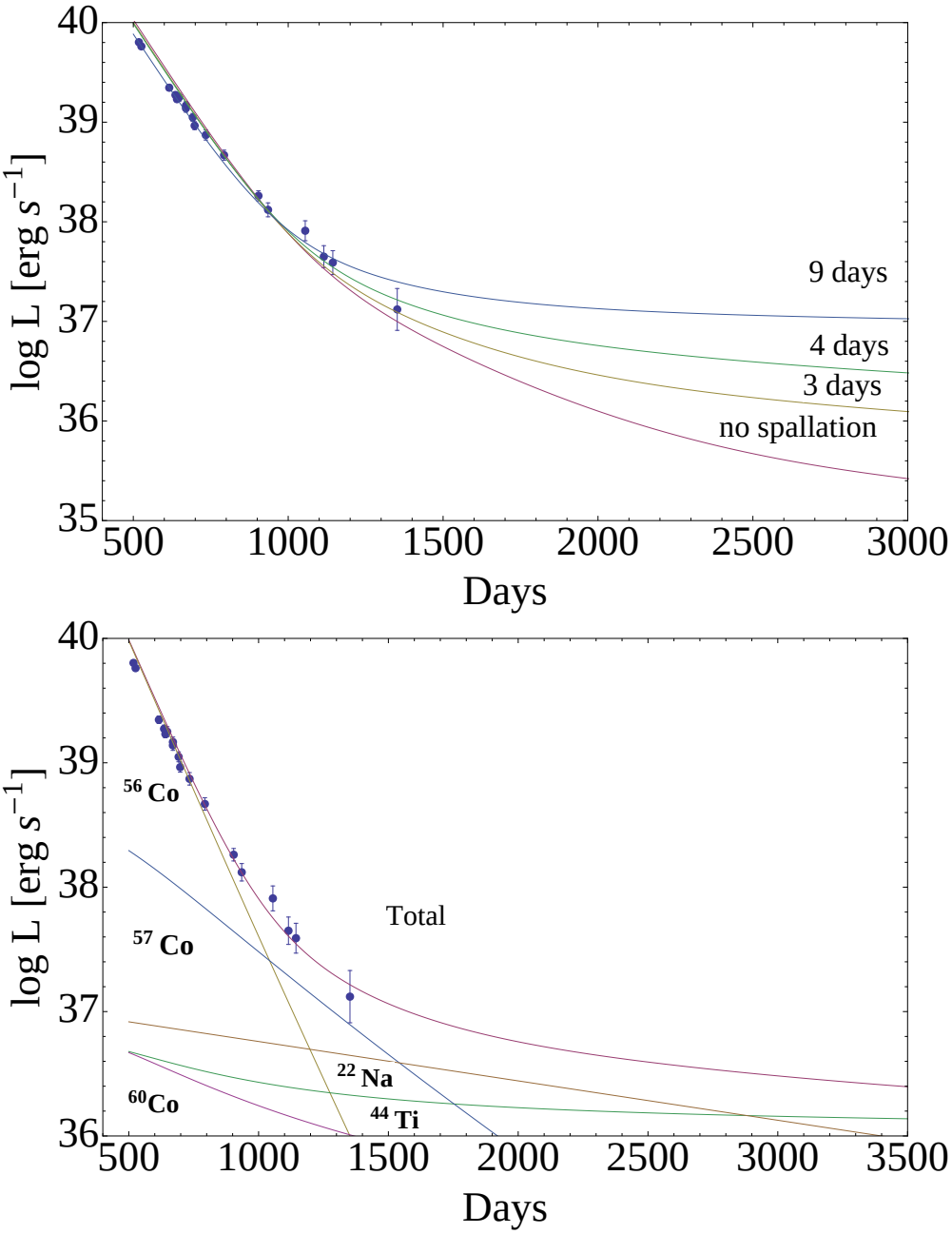

Figure 2.2: The SN1987A data comes from Suntzeff *et al.* (1991). The time delays represented in the upper panel are $t_{\rm delay} = 3, 4$ and 9 days. In the upper panel we also depict the original $M_{\rm Ni} = 0.1$ M$_\odot$ target without the spallation, where luminosity contributions of ^{57}Co and ^{60}Co were added artificially, and their values, 5.5×10^{-3} M$_\odot$ and 1.14×10^{-5} M$_\odot$, respectively, were taken from Woosley *et al.* (1995). The points are the SN 1987A data and the solid lines indicate our model. The y-axis is the logarithm of luminosity in units of erg/sec. In the lower plot, we also include the individual luminosity contributions of each isotope, where the contributions of ^{57}Co and ^{60}Co were artificially constructed in identical fashion to the upper panel. The masses of ^{56}Ni, ^{22}Na and ^{44}Ti, are actual, spallation products of our model. For $t_{\rm delay} = 4$ days, the values are 0.99 M$_\odot$, 5.50×10^{-5} M$_\odot$, and 1.20×10^{-4} M$_\odot$, respectively.

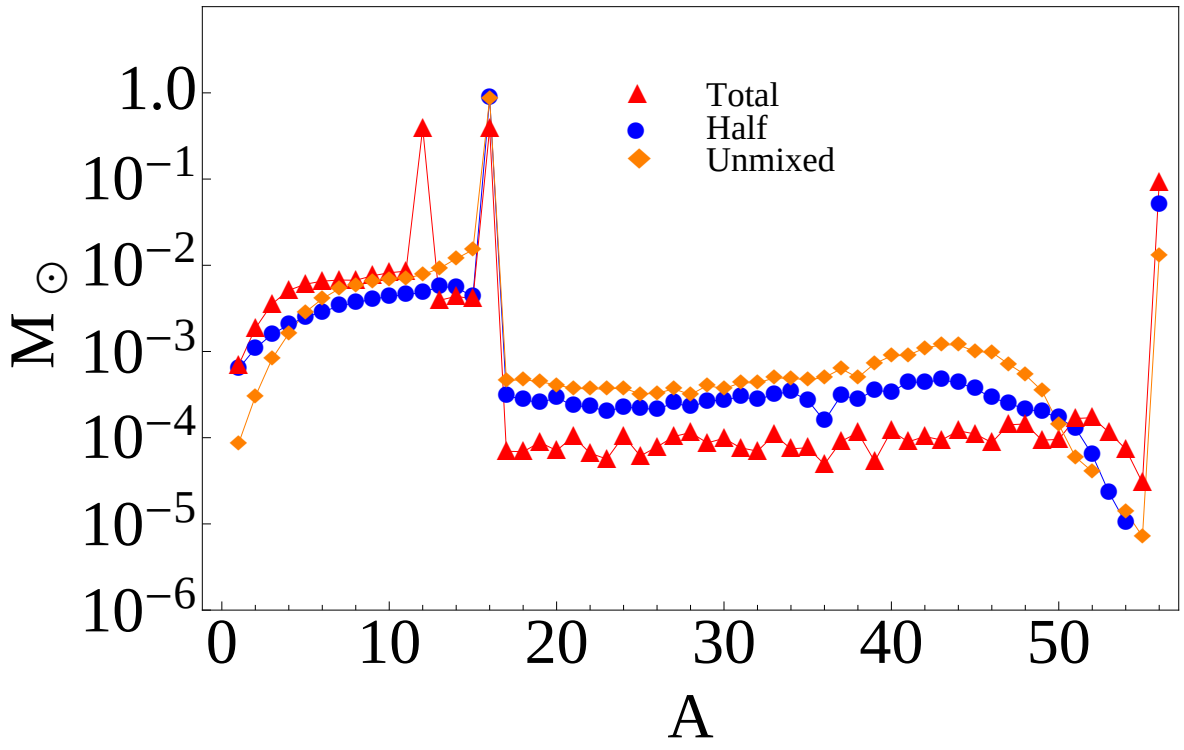

Figure 2.3: Mass in $M_\odot$ of isotopes of a particular atomic mass number produced by our spallation model at a $t_{\text{delay}} = 4$ days, for the three different mixed states. The x-axis represents the mass number A, and the y-axis represents the mass of nucleus of mass number A.

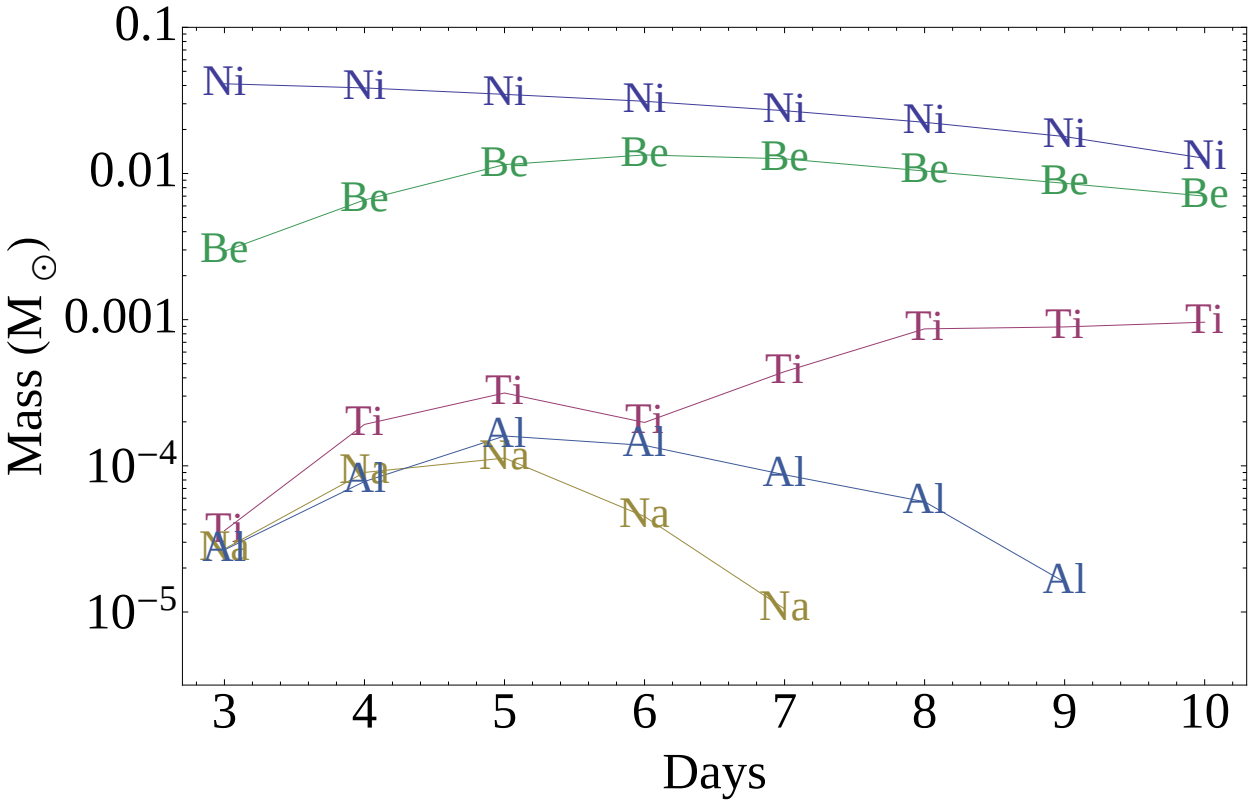

Figure 2.4: Mass yields of ^{56}Ni, ^{44} Ti, ^{22}Na, ^{26}Al and ^{7}Be, where x-axis represents $t_{\rm delay}$ and the y-axis represents the mass in units of $M_\odot$. The panel depicts the yields for spallation of the inner ~ 1.0 $M_\odot$ of the SN ejecta.

2.3.2 Isotope Abundance

Our spallation model creates isotopes of almost every mass number in the range of $A < 56$. However, very few of the isotopes created can be detected with γ-ray telescopes, because the SN envelope only becomes transparent to nuclear decay radiation after a time period of at least months (Diehl, 2012), so only isotopes that have a half life of at least in the order of weeks will have detectable nuclear decay lines. Therefore, in Fig 2.4, we only include the masses of isotopes with half lives of at least in the order of weeks.

In Fig. 2.3 and 2.4 we plot some of the trends of these isotopes. We notice that in Fig. 2.3, the model produces more mass for light isotopes than heavier isotopes. This is caused by the spallation of C and O. We also notice that the plots in Fig. 2.3 are divided in roughly two plateaus, where their boundary is in $A \sim 16$, which is the atomic mass number of Oxygen. We observe that for $A < 6$, the unmixed target produces the least amount of mass. Spallation of C and O enhances the production of light isotopes, yet, in the unmixed state, O and C are shielded by the Ni layer. Therefore, only spallation neutrons that manage to traverse the Ni layer will be able to interact with the O layer (At $t_{\rm delay} = 4$ days spallation neutrons do not reach the C layer in the unmixed state). We also notice that the two sides divided by $A \sim 16$ represent opposing trends. In $A < 16$, the total mixed state produces the most mass, while sometimes half-mixed state produces more mass over the unmixed state, and viceversa. Yet, at $A > 16$, the unmixed state produces the most mass, followed by the half-mixed, with the mixed state producing the least mass. This hierarchy of production at $A > 16$ is created by the availability of ^{56}Ni for spallation neutrons. The more mixing the target experiences, the least amount of ^{56}Ni is spallated, and therefore the least amount of heavier isotopes created. In Fig. 2.4, which represents the mass trends for a total mixed state, we plot the mass of one of the lighter isotopes, ^{7}Be, which has a half life of 76 days, which gives enough time for nuclear decay photons to go through the SN photosphere. Compared to the models of Woosley *et al.* (1995), we notice that our model

produces more ^{7}Be and ^{22}Na. We also notice that ^{44}Ti, ^{56}Ni, and ^{26}Al are in the same order of magnitudes as other models (Woosley *et al.* , 1995). Finally, it seems we can constrain production of ^{22}Na and ^{26}Al at higher $t_{\rm delay}$, where ^{22}Na production ends at $t_{\rm delay} \sim 7$ and ^{26}Al production at $t_{\rm delay} \sim 8$ days.

2.4 Discussion and Predictions

- *^{44}Ti production as a dsQN specificity and SN1987A:* We argue that the rarity of observations (The *et al.* , 2006) of ^{44}Ti might be related to the fact that ^{44}Ti is not produced by standard cc-SNe, but by dsQNe. In a recent paper (Ouyed *et al.* , 2011), we argued that CasA's ^{44}Ti lines were produced by a an unmixed dsQN through a significant ^{56}Ni depletion. Although, it is probably possible to avoid the excessive ^{56}Ni depletion in our original model by adjusting some parameters, and yet still predict a ^{44}Ti mass yield that is compatible with observations, it seems more natural and elegant to extend our model with mixing. Through total mixing, we can predict very minimal destruction of ^{56}Ni (Fig. 2.4) because ^{56}Ni is spread throughout the whole envelope as opposed to the assumption where it is all concentrated in the inner layers. If ^{56}Ni is spread throughout a wider volume, then less ^{56}Ni nuclei will be available in the inner layers as targets for QN neutrons. This minimal depletion leaves almost all the ~ 0.1 M$_{\odot}$ of ^{56}Ni intact. In Fig 2.2 we plotted the data of SN1987A against our model, where SN1987A is a SN where ^{44}Ti has been measured indirectly (Motizuki & Kumagai, 2004; Suntzeff *et al.* , 1992; Woosley & Hoffman, 1991) and recently directly (Grebenev *et al.* , 2012). At lower time delays, QN energy is mostly spent in PdV work (Leahy & Ouyed, 2008), therefore at a time delay of 4 days, our model could reproduce a similar luminosity to SN1987A . Current observations of SN1987A point to thorough mixing of SN

layers (Mueller *et al.* , 1991), which compares well to the assumptions about mixing done in our model. Although a traditional, no-spallation model for SN1987A makes a good fit for the light curve, the traditional model fails to account for the apparent sub-luminosity of CasA (Ouyed *et al.* , 2011), whereas both CasA and SN1987A have similar amounts of ^{44}Ti. This discrepancy in our model is explained through the fact that CasA can possibly be an unmixed dsQN and SN1987A-like objects a mixed dsQN. Recent papers have provided alternative arguments for the possibility of SN1987A compact remnant being a Quark Star (Chan *et al.* , 2009).

- ^{7}*Be abundance:* In Fig. 2.3 and 2.4, across all mixing space, a very large abundance of ^{7}Be is produced compared to current cc-SN models (Diehl & Timmes, 1998; Woosley *et al.* , 1995). Current core collapse SN models don't produce enough ^{7}Be to reach the photosphere before ^{7}Be decays. However, our model predicts $\sim 10^{-3}$ - 10^{-2} $M_{\odot}$ for ^{7}Be, which could be enough so that a significant amount of it reaches the photosphere and therefore be detected by γ-ray telescopes. The 487 keV photon released by the β-decay of ^{7}Be into ^{7}Li, is in the detectable energy range of current γ-ray telescopes (INTEGRAL, NuSTAR, etc.). The large abundance of ^{7}Be is due to the spallation of mixed O and C in the inner SN layers. This high abundance in our model indicates that only core collapse SN that evolve into dsQN will have a detectable gamma signature of ^{7}Be. Currently, Novae are the only possible sources of detectable, ^{7}Be photons because standard cc-SN are too optically thick (Diehl & Timmes, 1998). However our dsQN model can produce an alternative point source of ^{7}Be photons. Our model produces significant amounts of ^{7}Be across the three mixed states (Fig. 2.3). Finally, such a massive amount of ^{7}Be should create a signature in the bolometric light curve.If we assume Cassiopeia A was an

unmixed dsQN (Ouyed *et al.* , 2011), it should have emitted a ^{7}Be signature shortly after detonation.

- ^{22}*Na abundance:* A small ^{22}Na contribution is predicted in late time core collapse SN light curves (Woosley *et al.* , 1995). However, our spallation model generates a much larger amount of ^{22}Na than expected. This large yields of ^{22}Na are due to the spallation of ^{56}Ni into lighter nuclei. Current models (Woosley *et al.* , 1995) give a $\sim 10^{-6}$M$_{\odot}$ for ^{22}Na, while our spallation model can produce as much as $\sim 10^{-3}$M$_{\odot}$ (Fig 2.3). Furthermore, ^{22}Na has a half-life of 2.6 yr, and decays into an excited state of ^{22}Ne, releasing energetic radiation (Diehl & Timmes, 1998). That large amount generates enough radiation to create a noticeable signal in the late time light curve, as pictured in Fig 2.2. The decay of ^{22}Na emits a 1.275 MeV γ line that can be detected by current γ-ray telescopes. These signals of ^{22}Na abundant dsQN cannot be reproduced in current models for cc-SNe.

- *Some limitations of our model:* Some simplifications were made in our model. One of them concerns the structure of the SN ejecta. Here, we only include O, C and ^{56}Ni as targets (See, however Ouyed 2013b). Furthermore, O, C, and ^{56}Ni spread isotropically across space. This isotropic distribution allows us to model the spallation targets with statistical weights derived from the isotopic abundances. However, studies of CasA's remnants point to asymmetry in the detonation (e.g. Fesen *et al.* 2006).

  Another simplification is related to the nuclear processes in the SN ejecta. We did not touch upon nuclear electron capture, neutrino capture, and other nuclear decay processes. These processes might affect the Ti and Ni channels. However, the main ideas of our model, that ^{44}Ti can be produced from a minimal destruction of ^{56}Ni, that spallation of ^{56}Ni will lead to enrichment of ^{22}Na,

and that spallation of O, and C will lead to an excess of ^{7}Be, seem reasonable. ^{56}Ni transported into the outer layers would experience less spallation than inner layer ^{56}Ni - thus creating the possibility for either sub-luminous or non sub-luminous Ti-rich objects. While other limitations of our model exist, which are discussed in Ouyed *et al.* (2011), the model contains testable predictions for ^{22}Na and ^{7}Be enrichment.

Acknowledgments

This research is supported by an operating grant from the National Science and Engineer-ing Research Council of Canada (NSERC). We also thank N. Koning and M. Kostka for helpful discussion.

Chapter 3

Paper 2

We wrote this paper to introduce our nucleus-nucleus spallation model. In Paper 1, we merely explored the neutron-nucleus spallation side of the dsQN. However, the QN ejecta is not only composed of neutrons, but it is a site of r-process as well. Therefore, the QN ejecta will include heavy isotopes that were produced in the r-process. These heavy isotopes collide against the inner, ^{56}Ni ejecta of the cc-SN, generating nucleus-nucleus reactions. In this event, the r-process heavy isotopes fragment into smaller daughter nuclei. The QN ejecta by itself produces abundant $A > 130$ isotopes, but underproduces $A < 130$ nuclei. However, when these heavy isotopes fragment, abundant $A < 130$ isotopes are created, which might be able to explain the $A > 90$ isotope range. Therefore, the nucleus-nucleus spallation addition acts as an extension to the QN's r-process model. This $A > 90$ range is unable to be explained by conventional r-process models, which form a substantial part of the solar system's abundances.

Production of $90 < A < 130$ Isotopes from Heavy Ion Spallation in Dual Shock Quark Novae

Amir Ouyed[1], Rachid Ouyed[1], and Denis Leahy[1]

Department of Physics and Astronomy, University of Calgary, 2500 University Drive NW, Calgary, Alberta, T2N 1N4 Canada[1]

3.1 Introduction

Conventional theory suggests the bulk of isotopes heavier than ^{56}Fe are produced through neutron capture processes. Neutron capture process are divided into rapid-neutron capture (r-process), and slow-neutron capture (s-process). Although there is some consensus about the sites wherein the s-process takes place, there is no unambiguous consensus for the astrophysical sites where the r-process manifests (Arnould & Goriely, 2012).

The r-process is capable of producing heavier isotopes than the s-process, because the capture of neutrons in the r-process is much faster than the time it takes for a neutron to β decay into a proton. Therefore, it is believed that the bulk of $A > 90$ isotopes requires the r-process. Thus, in order to understand the chemical abundances of the heavier elements in the universe, it is imperative to either locate where the r-process takes place, or find a substitute for the r-process (Cowan & Thielemann, 2004).

Traditionally, the prime candidate for the r-process site has been the core-collapse Supernova (cc-SN)(Arnould & Goriely, 2012). It is theorized that such cataclysmic event could release the amount of neutrons and entropy necessary for the production of heavy elements. However, as it is of date, the core-collapse Supernova model faces many challenges. The first issue is that current simulations are only able to yield under-powered explosions in middle-range mass ($8 - 15$ $M_\odot$) supernovae, and under controversial conditions (Burrows, 2013). However, even in simulations where a cc-SN is detonated artificially, the cc-SN does not generate the sufficiently high entropy per baryon and neutron/proton ratio necessary for

the r-process to take place. More recently, it was argued that neutrino-driven winds ejected from the proto-neutron star could provide the sufficient entropy to trigger the r-process. Yet, recent simulations have been unable to provide the high-levels of entropy that are necessary (Roberts *et al.* , 2010).

The second most popular candidate is the the Neutron Star Merger (NSM). The argument is that the decompressing neutron-crusts become a site with a high neutron-density, which is appropriate for the r-process. However, NSMs happen at a relatively late stage of the universe's evolution, therefore they are unable to explain the r-process enrichment of old, metal-poor stars (Jaikumar *et al.* , 2007). Furthermore, NSM's mass yield for elements lighter than $A \sim 120$ is too low in comparison with solar abundances (Korobkin *et al.* , 2012).

.

More recently, the Quark Nova (QN) was postulated as an alternative site for r-process nucleosynthesis (Jaikumar *et al.* , 2007). The Quark-Nova is the name given to the explosive phase transition from a spin-down neutron star to a quark-star (Ouyed *et al.* , 2002). The hot, and neutron-dense matter ejected by this detonation was suggested as an ideal site for the r-process(Ouyed *et al.* , 2002). One of the advantages the QN model offers, is that its r-process mass yield is consistent with the Galactic r-process yield (Jaikumar *et al.* , 2007). Furthermore, QNe can happen early in the Universe, which is consistent with the r-process signature of metal poor stars (Jaikumar *et al.* , 2007). However, the QN model in Jaikumar *et al.* (2007) underproduces isotopes in the $A < 130$ range, leaving the $90 < A < 130$ solar abundances unexplained.

The QN is also a feasible site for other processes of nucleosynthesis that are not the r-process. Ouyed *et al.* (2011) argued that the QN's ejected, neutron-dense matter, can interact with the ejecta of the prior cc-SN explosion. This interaction was hereby called the dual-shock Quark Nova (dsQN). These papers showed that the dsQN becomes a unique site

of spallation reactions, where the neutrons ejected in the QN spallate against the isotopes of the cc-SN ejecta, creating a nucleosynthesis mechanism (Ouyed *et al.* , 2011). This spallation nucleosynthesis was used to explain the sub-luminous but Ti-rich nature of Cassiopeia A. However, this spallation process only creates sub-Ni elements, which does not address the aforementioned $90 < A < 130$ gap.

We believe that the $90 < A < 130$ range can be explained with the dsQN model, with an additional correction. If the QN ejecta produces r-process heavy isotopes in the range of $A \geq 130$, then these heavy isotopes must collide against the cc-SN ejecta in the context of the dsQN. This collision fragments the QN's $A \geq 130$ beam, creating a rare-isotope beam of $A \leq 130$ elements. The fragments in the $A \leq 130$ isotope beam effectively bridges the $90 < A < 130$ gap. Therefore, $90 < A < 130$ elements are not created by the r-process, but the rare-isotope beam.

3.2 Model

We use a similar model to (Ouyed *et al.* , 2011), but for nucleus-nucleus reactions. The reaction cross sections are calculated by using parameterized, partial cross sections for proton-nucleus reactions (Silberberg *et al.* , 1998), and scaling the proton-nucleus cross sections into nucleus-nucleus cross sections through the algorithm of Tsao *et al.* (1993). We also use parameterized, total inelastic reaction cross-sections, which are taken from Sihver *et al.* (1993). In order to visualize the model, we make use of particle accelerator analogies, wherein the experiment is divided into a beam, and a target.

3.2.1 Initial Beam

According to past studies (Keränen *et al.* , 2005; Ouyed *et al.* , 2005a), an exploding neutron star can eject its outer most layers as a mass of $M_{QN} \sim 10^{-3}$ $M_{\odot}$. This neutron-rich ejecta becomes a site for r-process synthesis (Jaikumar *et al.* , 2007). The r-process generates a

heavy isotope beam, which we model as a pulse of ^{130}Ba nuclei, with a mass of $M_{\rm Ba} \sim 10^{-5}$ $M_\odot$. The beam has an energy of $E \sim 10$ GeV/u.

3.2.2 Target

The supernova, inner shell is modelled as the target. The inner shell is a Ni layer, with a mass 0.1 $M_\odot$ of ^{56}Ni. The shell is spherical, and expands with an inner radius of $R = v_{\rm sn} \times t_{\rm delay}$, where $v_{\rm sn} = 5000$ km/s is the speed of the SN ejecta, and t_{delay} is the time delay between the first cc-SN detonation, and the subsequent, QN detonation. The target's number density in the Ni layer is approximately constant, at $n = N_{\rm Ni}/(4\pi R^2 \Delta R)$, where $N_{\rm Ni}$ is the total number of ^{56}Ni nuclei, and ΔR is the Ni layer's thickness.

3.2.3 Collision Statistics

The probability that an inelastic collision between projectile specie i and target specie j, produces fragment of specie k is

$$P \approx \frac{\sigma_{i\to k}(Z_i, A_i, Z_j, A_j, Z_k, A_k, E)}{\sigma_{{\rm total},ij}(Z_i, A_i, Z_j, A_j)} \tag{3.1}$$

,

where $\sigma_{i\to k}$ is the partial reaction cross section for the fragmentation of projectile i into fragment k. The total inelastic reaction cross section for projectile i and target j, is $\sigma_{{\rm total},ij}$. Because all target particles are ^{56}Ni nuclei and the projectiles' energies are really large, the cross sections only vary across projectile space and fragment space, so $\sigma_{i\to k}(Z_i, A_i, Z_j, A_j, Z_k, A_k, E) \to \sigma_{i\to k}(Z_i, A_i, Z_k, A_k)$, and $\sigma_{{\rm total},ij}(Z_i, A_i, Z_j, A_j) \to \sigma_{{\rm total},i}(Z_i, A_i)$. The number N of nuclei k synthesized in the collision is,

$$N_k \approx \frac{\sigma_{i\to k}}{\sigma_{\text{total},i}} N_i \tag{3.2}$$

.

We assume that very little energy gets transferred in the collision, so the projectile fragments, conserve the same $E \sim 10$ GeV/u, and the target's fragments remain in their original place. The cross-sections are calculated in the projectile's rest frame, so in order to calculate target fragmentation, we switch to the target rest-frame and the formulas become identical.

We divide the target slab radially into virtual layers. Because the projectile beam is modelled as a pulse, all projectiles collide against target nuclei simultaneously at each of the individual layers. When the beam collides against a layer, the projectile beam fragments into smaller projectiles. We define an average, free path $\overline{\lambda}$ as a radial separation between the layers,

$$\overline{\lambda} = \frac{1/n \sum_i N_i/\sigma_{\text{total},i}}{\sum_i N_i} \tag{3.3}$$

,

where i is summed across all projectile species. The average, free path $\overline{\lambda}$ is calculated for each individual virtual layer. After the projectile beam collides with a layer, the average displacement of the beam becomes,

$$x = \sum_q \overline{\lambda}_q \tag{3.4}$$

where q is summed across all virtual layers traversed by the beam. The simulation stops when the displacement becomes larger than the width of the slab, that is, when the $x \leq \Delta R$ condition fails to be met.

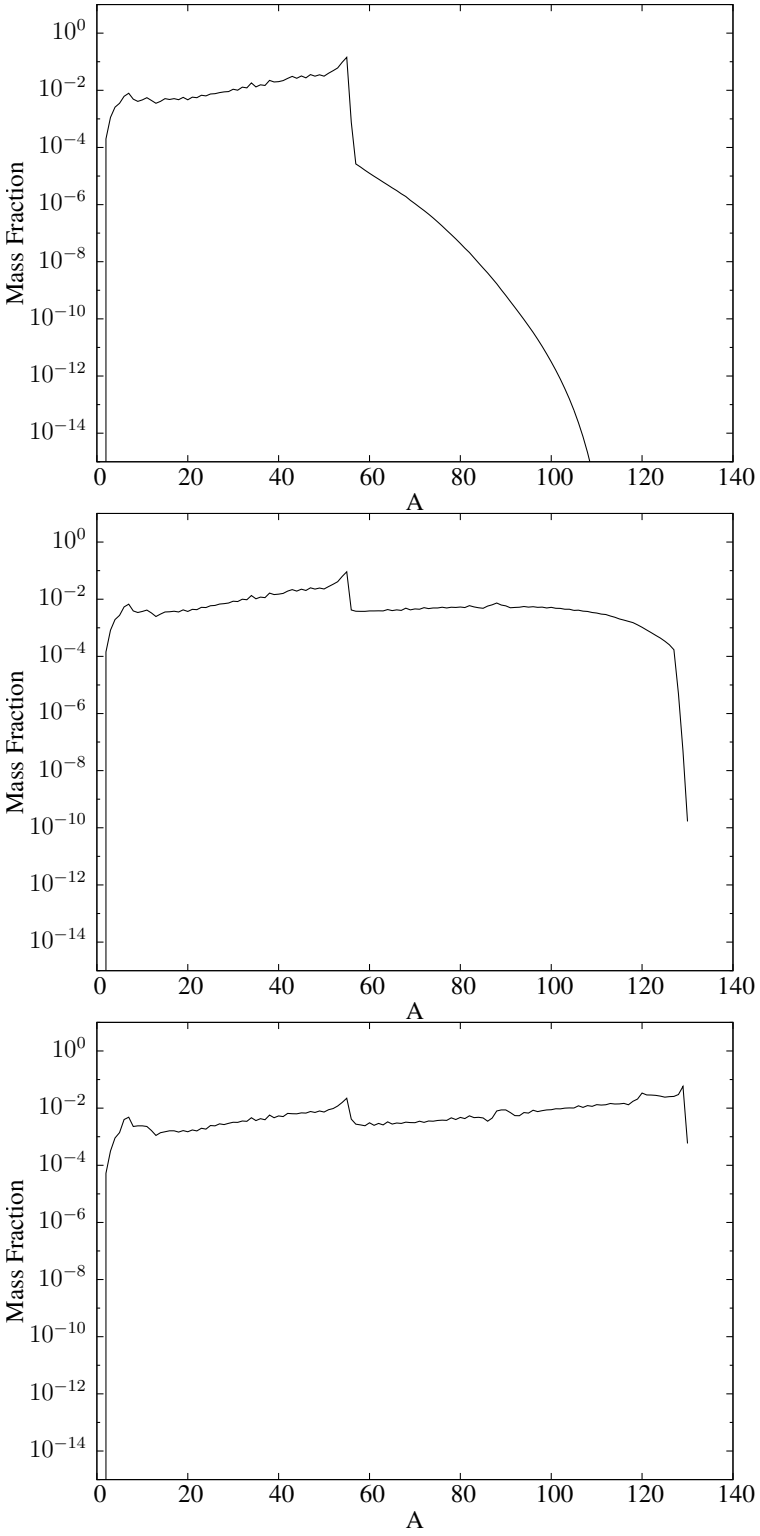

Figure 3.1: Mass fractions produced by the r-isotope beam process, as a function of A. From top to bottom, the time delays for the plots are $t_{\text{delay}} = 1, 3, 6$ days, consecutively.

3.3 Results

In Fig. 3.1, the mass yield is roughly divided along $A \sim 56$. The fragments of ^{56}Ni nuclei dominate the left side, and projectile fragments of ^{130}Ba dominate the right side.

Furthermore, the projectile breaks into larger fragments, as $t_{\rm delay}$ increases. The smaller the $t_{\rm delay}$ is, the denser the the SN-ejecta becomes, and therefore, the larger the number of virtual-layers that impact the beam. If a large amount of virtual layers impact the beam, the projectiles fragment into small nuclei. The opposite is true: a large $t_{\rm delay}$ leads to a low density target and a small number of virtual-layers, and therefore, large fragments.

Roughly, the opposite trend happens with $A \leq 56$ isotopes: larger $t_{\rm delay}$ means smaller fragments, and vice versa. A large $t_{\rm delay}$ fragments the ^{56}Ni into smaller nuclei because at such time delay values, projectile fragments are large, inflicting more energy into the targets. However, the effect in $A \leq 56$ is much less pronounced than $A \geq 56$.

At $t_{\rm delay} \geq 7$ days, the nucleus-nucleus reactions rapidly decrease, because the average free path becomes larger than the ΔR thickness of the Ni layer.

3.4 Discussion

- Elements not produces by r-process: Elements in the $90 \leq A \leq 130$ range are not created by r-process, but by rare-isotope beams. This has some very important consequences. First, this result implies that perhaps, the difficulty of producing $90 \leq A \leq 130$ in either the old QN or NSM model is due to an incompleteness - namely, the lack of a rare-isotope mechanism. Second, the astrophysical rare-isotope beam becomes an an important, novel nucleosynthesis mechanism, never theorized before.

- Robustness in relation to Ni-synthesis: The r-process yield is in the order of $\sim 10^{-5} - 10^{-3}$ M$_\odot$, which is much smaller compared to the ~ 0.1 M$_\odot$ mass of

the Ni layer. These large difference in magnitudes implies that the r-process beam will destroy only a trace amount of Ni, leaving the $\sim$ 0.1 $M_{\odot}$ figure almost intact. This makes our model, compatible with current light curve measurements (Woosley & Hoffman, 1991), and stellar nucleosynthesis models (Woosley *et al.* , 1995). In short, the trace Ni destruction gives our model a degree of universality.

- Robustness in relation to age of the Universe: Studies have shown that old, metal-poor stars, contain an overabundance of r-process elements in comparison to their Fe-peak elements, yet their r-process elements follow the solar abundance pattern(Sneden *et al.* , 2003). This implies that the r-process is invariant across different quantities of Fe-peak seeds, and thus, across the age of the Universe. The dsQN picture utilizes $A > 130$ projectiles as sources for the synthesis of $90 < A < 130$ isotopes, not Fe-peak seeds. Thus, the dsQN's production of $90 < A < 130$ isotopes is unaffected by the evolution of Fe-peak abundances in stars.

- Compatibility with r-process mass yield: Past studies show that the QN rate of event and is mass yield is compatible with the galactic r-process mass yield (Jaikumar *et al.* , 2007). It follows, then that the rare-isotope beam inherent to the dsQN might be roughly compatible as well.

- Challenges and future work: It is necessary to make a detailed, quantitative comparison of the rare-isotope beam abundances with solar abundances. Furthermore, its important to describe discriminating, astronomical signatures for the rare-isotope beam process - for example, finding rare-isotope beam elements that cannot be created in r-process.

Acknowledgments

This research is supported by an operating grant from the National Science and Engineering Research Council of Canada (NSERC).

Chapter 4

Summary and Conclusion

Our spallation-nucleosynthesis model - the dual shock Quark Nova - is the first of its kind. Most nucleosynthesis models are based on particle accretion - that is, nuclei and small particles merge together to create a larger daughter nucleus. Nuclear spallation is the opposite - it fragments larger nuclei into smaller particles. While nuclear spallation has an astrophysical role outside dsQNe, its role is mainly confined to cosmic ray spallation. Furthermore, the nucleosynthetic properties of cosmic ray spallation are limited to the creation a few isotopes, while the dsQN model can produce an extensive range of isotopes. Moreover, the dsQN is not only a site of nucleon-nucleus spallation, but of heavy ion spallation as well. The fragmentation of $A > 130$ isotopes is not seen anywhere in astronomy except in the dsQN's heavy ion collisions. In short, our spallation model gives an astrophysical dimension to physical mechanisms that were mostly confined to cutting edge labs -e.g. CERN and rare-isotope facilities.

Furthermore, the dsQN spallation model is not only valuable for its novelty, but also for its explanatory properties. Spallation in the dsQN might be the solution behind the peculiar case of ^{44}Ti production (1.1.1). The dsQN could explain the production of ^{44}Ti in core collapse supernovae as a natural consequence of the spallation of ^{56}Ni by QN neutrons. This destruction of ^{56}Ni could in turn, bring on as consequence the large ^{44}Ti/^{56}Ni ratio detected in some cc-SNe. In addition, the lack of detected ^{44}Ti point sources in the sky follows naturally from the constraints set upon by the dsQNe. ^{44}Ti is an important isotope in astrophysics, both theoretically, and observationally, and therefore, a consistent explanation for its production will have important consequences.

The dsQN might be also the missing piece to the r-process puzzle (1.1.2). Conventional

theory suggests that $A > 90$ isotopes are mostly created through the r-process. However, conventional models for the production of these isotopes face many challenges. Without a site for the production of $A > 90$ isotopes, a substantial part of the abundances in the solar system are left unexplained. Yet, the dsQN seems like a good candidate for the production of these isotopes. Older work demonstrated that the QN can create fairly heavy $A > 130$ isotopes through the r-process, but it underproduced $A < 130$ elements. However, the spallation of the dsQN can fragment the r-process' $A > 130$ nuclei, producing abundant $A < 130$ isotopes, effectively correcting the older, QN r-process model. Thus, the r-process triggered in the QN, coupled with our novel, spallation model, could explain the origin of $A > 90$ isotopes.

Moreover, the dsQN is fairly robust, for its universality is compatible with many astronomical observations. One example of its universality is related to ^{44}Ti production. The dsQN can still produce a large ^{44}Ti signature in objects with large amount of ^{56}Ni, which makes the dsQN model compatible with other objects beyond the sub-luminous, Ni-deficient Cassiopeia A. Mixing in the SN layers can attenuate the destruction of ^{56}Ni, without changing much the production of abundant ^{44}Ti. Therefore, mixing could explain why supernova-like objects that are not sub-luminous, can still show a strong ^{44}Ti signature (i.e. SN1987A). Moreover, the dsQN is universal across the universe's lifetime. The dsQN can be triggered early in the universe, which could in turn produce the r-process signatures found in old, metal-poor stars. In addition, our spallation nucleosynthesis model does not depend on Fe seeds, which makes it universal across the evolution of metallicity in stars. Research has shown that r-process signatures are fairly similar across stars with different fractional abundances of Fe - which is problematic to the r-process. The r-process utilizes Fe seeds to create heavier isotopes, and thus, different abundances of Fe should yield different r-process signatures - which stands in contrast with the invariant r-process signatures across metallicity.

Finally, dsQN spallation produces unique signatures that could aid in its detection. A

remarkable signature is the large abundance of radioactive ^{7}Be produced by neutron-Ni spallation - which can be detected with a γ-ray telescope.

Future work should be spent in the fine-tuning of this spallation nucleosynthesis model. Our model for the propagation of the nuclear cascade is very qualitative. A more precise, quantitative model would solve the appropriate differential equations for the spatial and temporal propagation of the nuclear cascade. Furthermore, a better understanding of the transition from hadronic to strange quark matter would constrain the currently free parameter of $t_{\rm delay}$. In order to develop a better understanding of this transition, more work needs to be done on the nature of the spin-down evolution of neutron stars, and the burning of hadronic matter into strange matter.

In conclusion, not only is the dsQN (and consequently, the QN) a fascinating mechanism in its own right, but if its existence is accepted, then the dsQN could answer important questions in the scientific community.

Bibliography

Aad, Georges, Abbott, B, Abdallah, J, Abdelalim, AA, Abdesselam, A, Abdinov, O, Abi, B, Abolins, M, Abramowicz, H, Abreu, H, *et al.* . 2010. Observation of a Centrality-Dependent Dijet Asymmetry in Lead-Lead Collisions at $\sqrt{s_{\rm NN}} = 2.76$ TeV with the ATLAS Detector at the LHC. *Physical review letters*, **105**(25), 252303.

Andronic, A, Braun-Munzinger, P, Redlich, K, & Stachel, J. 2003. Statistical hadronization of charm in heavy-ion collisions at SPS, RHIC and LHC. *Physics Letters B*, **571**(1), 36–44.

Arnould, Marcel, & Goriely, Stéphane. 2012. The r-process of nucleosynthesis: The puzzle is still with us. *Chapitre 4*.

Burbidge, E. Margaret, Burbidge, G. R., Fowler, William A., & Hoyle, F. 1957. Synthesis of the Elements in Stars. *Rev. Mod. Phys.*, **29**(Oct), 547–650.

Burrows, Adam. 2013. *Colloquium* : Perspectives on core-collapse supernova theory. *Rev. Mod. Phys.*, **85**(Feb), 245–261.

Chan, TC, Cheng, KS, Harko, T., Lau, HK, Lin, LM, Suen, WM, & Tian, XL. 2009. Could the compact remnant of SN 1987A be a quark star? *The Astrophysical Journal*, **695**, 732.

Clayton, DD, Jin, L, Meyer, BS, *et al.* . 1998. Nuclear Reactions Governing the Nucleosynthesis of ^{44}Ti. *The Astrophysical Journal*, **504**(1), 500.

Clayton, Donald D. 1971. New Prospect for Gamma-Ray-Line Astronomy.

Cowan, John J, & Thielemann, Friedrich-Karl. 2004. R-process nucleosynthesis in supernovae. *Physics Today*, **57**(10), 47–54.

Cugnon, J., Volant, C., & Vuillier, S. 1997. Nucleon and deuteron induced spallation reactions. *Nuclear Physics A*, **625**(4), 729–757.

Diehl, R. 2012. Nucleosynthesis and Gamma-Ray Line Spectroscopy with INTEGRAL. *Arxiv preprint arXiv:1202.0481*.

Diehl, R., & Timmes, F.X. 1998. Gamma-Ray Line Emission from Radioactive Isotopes in Stars and Galaxies. *Publications of the Astronomical Society of the Pacific*, **110**(748), 637–659.

Fesen, R.A., Hammell, M.C., Morse, J., Chevalier, R.A., Borkowski, K.J., Dopita, M.A., Gerardy, C.L., Lawrence, S.S., Raymond, J.C., & van den Bergh, S. 2006. The expansion asymmetry and age of the Cassiopeia A supernova remnant. *The Astrophysical Journal*, **645**, 283.

Filges, Detlef, & Goldenbaum, Frank. 2010. Handbook of Spallation Research: Theory, Experiments and Applications. *Handbook of Spallation Research: Theory, Experiments and Applications by Detlef Filges and Frank Goldenbaum. Wiley, 2010. ISBN: 978-3-527-40714-9*, **1**, 3–61.

Görres, J, Meißner, J, Schatz, H, Stech, E, Tischhauser, P, Wiescher, M, Bazin, D, Harkewicz, R, Hellström, M, Sherrill, B, *et al.* . 1998. Half-Life of ^{44}Ti as a Probe for Supernova Models. *Physical review letters*, **80**(12), 2554.

Gosse, John C, & Phillips, Fred M. 2001. Terrestrial in situ cosmogenic nuclides: theory and application. *Quaternary Science Reviews*, **20**(14), 1475–1560.

Grebenev, SA, Lutovinov, AA, Tsygankov, SS, & Winkler, C. 2012. Hard-X-ray emission lines from the decay of ^{44}Ti in the remnant of supernova 1987A. *Nature*, **490**(7420), 373–375.

Hachisu, I., Matsuda, T., Nomoto, K., & Shigeyama, T. 1991. Rayleigh-Taylor instabilities and mixing in the helium star models for Type Ib/Ic supernovae. *The Astrophysical Journal*, **368**, L27–L30.

Hüfner, J. 1985. Heavy fragments produced in proton-nucleus and nucleus-nucleus collisions at relativistic energies. *Physics Reports*, **125**(4), 129–185.

Hwang, U., & Laming, J.M. 2012. A Chandra X-Ray Survey of Ejecta in the Cassiopeia A Supernova Remnant. *The Astrophysical Journal*, **746**, 130.

Iyudin, AF, Diehl, R., Bloemen, H., Hermsen, W., Lichti, GG, Morris, D., Ryan, J., Schoenfelder, V., Steinle, H., Varendorff, M., *et al.* . 1994. COMPTEL observations of ^{44}Ti gamma-ray line emission from CAS A. *Astronomy and Astrophysics*, **284**, L1–L4.

Jaikumar, P, Meyer, BS, Otsuki, K, & Ouyed, R. 2007. Nucleosynthesis in neutron-rich ejecta from quark-novae. *Astronomy and Astrophysics*, **471**(1), 227–236.

Jordan, George C., Gupta, Sanjib S., & Meyer, Bradley S. 2003. Nuclear reactions important in α-rich freeze-outs. *Phys. Rev. C*, **68**(Dec), 065801.

Käppeler, F., Gallino, R., Bisterzo, S., & Aoki, Wako. 2011. The *s* process: Nuclear physics, stellar models, and observations. *Rev. Mod. Phys.*, **83**(Apr), 157–193.

Keränen, P., Ouyed, R., & Jaikumar, P. 2005. Neutrino emission and mass ejection in quark novae. *The Astrophysical Journal*, **618**, 485.

Kifonidis, K., Plewa, T., Janka, H.T., & Müller, E. 2000. Nucleosynthesis and clump formation in a core-collapse supernova. *The Astrophysical Journal Letters*, **531**, L123.

Korobkin, O, Rosswog, Stephan, Arcones, A, & Winteler, C. 2012. On the astrophysical robustness of the neutron star merger r-process. *Monthly Notices of the Royal Astronomical Society*, **426**(3), 1940–1949.

Kostka, Mathew, Koning, Nico, Ouyed, Rachid, Leahy, Denis, & Steffen, Wolfgang. 2012. Quark Nova Signatures in Super-luminous Supernovae. *arXiv preprint arXiv:1206.7113*.

Krása, Antonın. 2010. *Spallation Reaction Physics*.

Leahy, D., & Ouyed, R. 2008. Supernova SN2006gy as a first ever Quark Nova? *Monthly Notices of the Royal Astronomical Society*, **387**(3), 1193–1198.

Leibundgut, B., & Suntzeff, N. 2003. Optical light curves of supernovae. *Supernovae and gamma-ray bursters*, 77–90.

Letaw, J.R., Silberberg, R., & Tsao, CH. 1983. Proton-nucleus total inelastic cross sections-an empirical formula for E greater than 10 MeV. *The Astrophysical Journal Supplement Series*, **51**, 271–275.

Limongi, M., & Chieffi, A. 2006. Nucleosynthesis in Core Collapse Supernovae. *Pages 99–104 of: Origin of Matter and Evolution of Galaxies*, vol. 847.

Magkotsios, Georgios, Timmes, Francis X, Hungerford, Aimee L, Fryer, Christopher L, Young, Patrick A, & Wiescher, Michael. 2010. Trends in ^{44}Ti and ^{56}Ni from Core-collapse Supernovae. *The Astrophysical Journal Supplement Series*, **191**(1), 66.

Mashnik, Stepan G. 2000. On solar system and cosmic rays nucleosynthesis and spallation processes. *arXiv preprint astro-ph/0008382*.

Motizuki, Y., & Kumagai, S. 2004. Radioactivity of the Key Isotope ^{44}Ti in SN 1987A. *Pages 369–374 of: Tours Symposium on Nuclear Physics V*, vol. 704.

Mueller, E., Fryxell, B., & Arnett, D. 1991. Instability and clumping in SN 1987A. *Astronomy and Astrophysics*, **251**, 505–514.

Nagataki, Shigehiro, Hashimoto, Masa-Aki, Sato, Katsuhiko, Yamada, Shoichi, & Mochizuki, Yuko S. 1998. The high ratio of ^{44}Ti/^{56}Ni in Cassiopeia A and the axisymmetric collapse-driven supernova explosion. *The Astrophysical Journal Letters*, **492**(1), L45.

Niebergal, B., Ouyed, R., & Jaikumar, P. 2010. Numerical simulation of the hydrodynamical combustion to strange quark matter. *Physical Review C*, **82**(6), 062801.

Niebergal, B. P. 2007. *A new model for soft gamma-ray repeaters and anomalous x-ray pulsars using quark stars*. Ph.D. thesis, University of Calgary, Canada.

Ouyed, R. 2013a. A new model for the origin of very metal poor stars and their chemical composition. *Monthly Notices of the Royal Astronomical Society*, **428**(Jan.), 236–253.

Ouyed, R. 2013b. A resolution of the cosmic Lithium problem. *ArXiv e-prints*, Apr.

Ouyed, R., & Leahy, D. 2012. The peculiar case of the "double-humped" super-luminous supernova SN2006oz. *arXiv preprint arXiv:1202.2400*.

Ouyed, R., Dey, J., & Dey, M. 2002. Quark-Nova. *Astronomy and Astrophysics*, **390**(3), 39–42.

Ouyed, R., Rapp, R., & Vogt, C. 2005a. Fireballs from quark stars in the color-flavor locked phase: application to gamma-ray bursts. *The Astrophysical Journal*, **632**, 1001.

Ouyed, R, Keränen, P, & Maalampi, J. 2005b. Ultra-high-energy cosmic rays from hypothetical quark novae. *The Astrophysical Journal*, **626**(1), 389.

Ouyed, R., Leahy, D., Ouyed, A., & Jaikumar, P. 2011. Spallation Model for the Titanium-Rich Supernova Remnant Cassiopeia A. *Physical Review Letters*, **107**(15), 151103.

Ouyed, R., Kostka, M., Koning, N., Leahy, D., & Steffen, W. 2012. Quark nova imprint in the extreme supernova explosion SN 2006gy. *Monthly Notices of the Royal Astronomical Society*, 1652–1662.

Ouyed, Rachid. 2013. A resolution of the cosmic Lithium problem. *arXiv preprint arXiv:1304.3715*.

Ouyed, Rachid, & Staff, Jan. 2013. Quark-novae in neutron star-white dwarf binaries: a model for luminous (spin-down powered) sub-Chandrasekhar-mass Type Ia supernovae? *Research in Astronomy and Astrophysics*, **13**(4), 435.

Ouyed, Rachid, Leahy, Denis, & Jaikumar, Prashanth. 2009a. Predictions for signatures of the quark-nova in superluminous supernovae. *arXiv preprint arXiv:0911.5424*.

Ouyed, Rachid, Leahy, Denis, Staff, Jan, & Niebergal, Brian. 2009b. Quark-nova explosion inside a collapsar: application to Gamma Ray Bursts. *Advances in Astronomy*, **2009**.

Ouyed, Rachid, Pudritz, Ralph E, & Jaikumar, Prashanth. 2009c. Quark-Novae, cosmic reionization, and early r-process element production. *The Astrophysical Journal*, **702**(2), 1575.

Roberts, LF, Woosley, SE, & Hoffman, RD. 2010. Integrated nucleosynthesis in neutrino-driven winds. *The Astrophysical Journal*, **722**(1), 954.

Rudstam, G. 1966. *Systematics of spallation yields.* Tech. rept. CERN, Geneva.

Schatz, Hendrik. 2008. Rare isotopes in the cosmos. *Physics Today*, **61**, 40–45.

Serber, R_. 1947. Nuclear reactions at high energies. *Physical Review*, **72**(11), 1114.

Sihver, Lembit, Tsao, CH, Silberberg, R, Kanai, T, & Barghouty, AF. 1993. Total reaction and partial cross section calculations in proton-nucleus ($Z_t \leq 26$) and nucleus-nucleus reactions (Z_p and $Z_t \leq 26$). *Physical Review C*, **47**(3), 1225.

Silberberg, R, Tsao, CH, & Barghouty, AF. 1998. Updated partial cross sections of proton-nucleus reactions. *The Astrophysical Journal*, **501**(2), 911.

Sneden, Christopher, Cowan, John J, Lawler, James E, Ivans, Inese I, Burles, Scott, Beers, Timothy C, Primas, Francesca, Hill, Vanessa, Truran, James W, Fuller, George M, *et al.* . 2003. The extremely metal-poor, neutron capture-rich star CS 22892-052: a comprehensive abundance analysis. *The Astrophysical Journal*, **591**(2), 936.

Staff, Jan E, Ouyed, Rachid, & Jaikumar, Prashanth. 2006. Quark deconfinement in neutron star cores: the effects of spin-down. *The Astrophysical Journal Letters*, **645**(2), L145.

Staff, Jan E, Jaikumar, Prashanth, Chan, Vincent, & Ouyed, Rachid. 2012. Spindown of Isolated Neutron Stars: Gravitational Waves or Magnetic Braking? *The Astrophysical Journal*, **751**(1), 24.

Suntzeff, N.B., Phillips, MM, Depoy, DL, Elias, JH, & Walker, AR. 1991. The late-time bolometric luminosity of SN 1987A. *The Astronomical Journal*, **102**, 1118–1134.

Suntzeff, N.B., Phillips, MM, Elias, JH, Walker, AR, & Depoy, DL. 1992. The energy sources powering the late-time bolometric evolution of SN 1987A. *The Astrophysical Journal*, **384**, L33–L36.

The, L.S., Clayton, DD, Diehl, R., Hartmann, DH, Iyudin, AF, Leising, MD, Meyer, BS, Motizuki, Y., & Schönfelder, V. 2006. Are Ti-producing supernovae exceptional? *Astronomy and Astrophysics*, **450**(3), 1037–1050.

Timmes, F.X. n.d.. *Supernova Light Curves' Codes for Cococubed*.

Tsao, CH, Silberberg, R, Barghouty, AF, Sihver, Lembit, & Kanai, T. 1993. Scaling algorithm to calculate heavy-ion spallation cross sections. *Physical Review C*, **47**(3), 1257.

Vink, Jacco, Laming, J Martin, Kaastra, Jelle S, Bleeker, Johan AM, Bloemen, Hans, & Oberlack, Uwe. 2001. Detection of the 67.9 and 78.4 keV lines associated with the radioactive decay of ^{44}Ti in Cassiopeia A. *The Astrophysical Journal Letters*, **560**(1), L79.

Weber, Fridolin. 2005. Strange quark matter and compact stars. *Progress in Particle and Nuclear Physics*, **54**(1), 193–288.

White, Marion M, *et al.* . 2002. Spallation neutron source (SNS). *Pages 15–24 of: AIP CONFERENCE PROCEEDINGS*. IOP INSTITUTE OF PHYSICS PUBLISHING LTD.

Witten, Edward. 1984. Cosmic separation of phases. *Physical Review D*, **30**(2), 272.

Woosley, SE, & Hoffman, R.D. 1991. ^{57}Co and ^{44}Ti production in SN 1987A. *The Astrophysical Journal*, **368**, L31–L34.

Woosley, S.E., Langer, N., & Weaver, T.A. 1995. The presupernova evolution and explosion of helium stars that experience mass loss. *The Astrophysical Journal*, **448**, 315.

York, RC, Bollen, G, Compton, C, Crawford, AC, Doleans, M, Glasmacher, T, Hartung, W, Marti, F, Popielarski, J, Vincent, JJ, *et al.* . 2009. FRIB: a new accelerator facility for the production of rare isotope beams. *Pages 888–894 of: International Conference on Radio Frequence Superconductivity.*